2015

Shear Capacity of RC Beams at Elevated Temperatures

Maged A. Youssef
Western University, youssef@uwo.ca

Mohamed Diab
The University of Western Ontario

Salah El-Din F. El-Fitiany
The University of Western Ontario

Prediction of the Shear Capacity of Reinforced Concrete Beams at Elevated Temperatures

M.A. Youssef [1,*], M. Diab [1], S.F. El-Fitiany [2]

[1] Department of Civil and Environmental Engineering, Western University, London, Ontario, Canada N6A 5B9
[2] Department of Structural Engineering, Alexandria University, Alexandria, Egypt.

Abstract

Fire safety is a critical criterion for designing reinforced concrete structures. With the introduction of performance based design, structural engineers need design tools to assess the capacity of different elements during fire exposure. This paper proposes an analytical method to predict the shear capacity of RC beams exposed to elevated temperatures. The proposed method extends the use of existing ambient temperature methods by accounting for the effect of elevated temperatures on material properties. It involves heat transfer analysis, evaluation of the material properties at elevated temperatures and application of the Modified Compression Field Theory to estimate the shear capacity. The method is validated using experimental results by others. A parametric study is then conducted to investigate the effects of different parameters on the shear capacity of RC beams exposed to fire.

Keywords

Reinforced concrete, elevated temperatures, heat transfer, fire resistance, shear capacity, beams.

---

* Corresponding author: Tel.: +1 (519) 661-2111x 88661; fax: +1 (519) 661-3779.
E-mail address: youssef@uwo.ca

1. Introduction

Reinforced Concrete (RC) is one of the most commonly used construction materials. It has advantages including strength, durability, and flexibility to be formed into irregular and complicated shapes. Concrete has also excellent characteristics with respect to fire resistance. It is non-combustible, and, thus does not propagate fire, nor produce toxic gases (Denoel, 2007). Its low thermal conductivity delays the increase of temperatures of the section's inner core and the reinforcing steel bars. Regardless of these benefits, concrete resistance to fire should not be taken for granted. Concrete undergoes complex reactions and changes when exposed to elevated temperatures. These changes reduces the concrete strength and increases the corresponding strains.

Fire resistance of RC structural elements can be determined either experimentally or analytically. The high cost of fire tests makes them unsuitable for regular design. Analytical methods include the Finite Element Method (FEM) (Kodur and Wang, 2004). It requires performing a coupled thermal-stress analysis, which cannot be easily performed by design engineers.

Currently, concrete structures are being designed for fire safety using prescriptive methods that are based on experimental investigations. These methods usually specify the minimum cross-section dimensions and clear cover to achieve specific fire ratings. They tend to be conservative and do not give engineers any design flexibility (Purkiss, 2007). As new codes are moving towards performance-based design, simplified methods are needed to facilitate the prediction of the load-carrying capacity of RC elements during exposure to elevated temperatures. El-Fitiany and Youssef (2009, 2010) developed and validated a sectional analysis method to predict the flexural and axial behavior of RC members exposed to fire conditions. Based on this method, they developed stress block factors for concrete beams exposed to fire (El-Fitiany and Youssef, 2011), a simplified analysis technique for continuous RC beams exposed to fire (El-Fitiany and Youssef, 2014a), and a

simplified technique to sketch the axial force-moment interaction diagram for RC sections exposed to fire (El-Fitiany and Youssef, 2014b).

Many researchers have studied the shear capacity of RC sections at ambient temperature (Vecchio and Collins, 1986 and 1988; Kotsovos GM and Kotsovos MD, 2013; Murty and PapaRao 2013 and others). However, the shear capacity for sections exposed to fire has not been thoroughly investigated. There is a clear lack of analytical methods that can assess the shear behavior of concrete elements exposed to fire (Bamonte et al., 2009). The provisions of the current design standards are set based on the flexural capacity of a structural member during fire and needs to be modified to account for the shear capacity at elevated temperatures.

The aim of this paper is to develop a reliable and simple method to estimate the reduced shear capacity of RC beams exposed to elevated temperatures. The method involves the use of heat transfer analysis to determine the temperatures within the cross-section and the Modified Compression Field Theory (MCFT) by Vecchio and Collins (1986) to predict the shear capacity. The paper also presents a parametric study to investigate the effects of various design parameters on the shear capacity of RC beams during exposure to fire.

2. Proposed method

The proposed method assumes that the shear capacity at elevated temperatures can be derived using existing ambient temperature methods while accounting for the effect of elevated temperatures on the materials (Masaad and Chefdebien, 2007). Figure 1 summarizes the main steps for this method, which include determining the temperature distribution within the studied cross-section, evaluating the reduced strength properties of concrete and steel bars, and calculating the shear resistance of the cross-section.

2.1 Heat transfer analysis

The temperature distribution within a concrete cross-section during exposure to fire includes the FEM, the Finite Difference Method (FDM) as well as many simplified methods. The FEM is the most general tool to predict the thermal distribution but it is time consuming. The FDM (Lie, 1992) is considered a simplified version of the FEM and is utilized in this paper to evaluate the temperature distribution within the studied sections.

The boundary conditions for the studied section including dimensions, number of exposed faces, and the fire duration are first defined. The section is then divided into 45^{o} mesh elements as shown in Figure 2. The temperature at the center of each element represents the temperature of the entire element. The thermal conductivity (k_c) and specific heat capacity (C_c) are assumed using the equations reported by Lie (1992). The incremental temperature increase at the surface of the cross-section is determined based on the relationship between the fire temperature and its duration. Part of the heat energy conveyed to the boundary elements is used to increase their temperatures while the remaining energy is transferred to the inner elements.

2.2 Properties of materials at elevated temperatures

Youssef and Moftah (2007) provided an assessment of the available models of the material properties of concrete and steel at elevated temperatures. Their recommended models are utilized in this paper and are summarized below.

2.2.1 Concrete compressive strength

Hertz's model (Hertz, 2005) is used to predict the reduced concrete compressive strength at elevated temperatures (f'_{cT}):

$$f'_{cT} = \frac{f'_c}{1 + \frac{T}{15,000} + \left(\frac{T}{800}\right)^2 + \left(\frac{T}{570}\right)^8 + \left(\frac{T}{100,000}\right)^{64}} \quad (1)$$

Where (T) is the temperature in degree Celsius, and (f'_c) is the concrete compressive strength at ambient temperature.

2.2.2 Concrete tensile strength

Youssef et al. (2008) recommend the use of Eq. 2 to predict the tensile strength of concrete at elevated temperature (f_{tT}).

$$f_{tT} = f_t \times \frac{f'_{cT}}{f'_c} \quad (2)$$

Where (f_t) is the concrete tensile strength at ambient temperature and can be defined using Eq. (3) by Bentz (2000).

$$f_t = 0.45 \times (f'_c)^{0.4} \quad (3)$$

2.2.3 Fire-induced strains in concrete

Total concrete strain at elevated temperatures (ε_{tot}) is the summation of three terms: instantaneous stress related strain (ε_{oT}), thermal strain (ε_{th}), and transient strain (ε_{tr}). This paper focuses on unrestrained elements, and, thus thermal strain does not have an effect. Transient strain is induced during the heating of concrete and is considered the largest component of the total strain.

Terro's model (1998), Eq. 4, is used to predict the transient strains at elevated temperatures.

$$\varepsilon_{tr} = \varepsilon_{03}\left(0.032 + 3.226\frac{f_c}{f_c^{'}}\right)\left(\frac{V_a}{0.65}\right) \tag{4}$$

Where, V_a is the volume of aggregate and

$$\varepsilon_{o3} = 43.87\times10^{-6} - 2.73\times10^{-8}T - 6.35\times10^{-8}T^2 + 2.19\times10^{-10}T^3 - 2.77\times10^{-13}T^4$$

2.2.4 Yield stress of Steel

The model presented by Lie (1992) is used to predict the reduced yield strength of reinforcement steel at elevated temperatures (f_{yT}):

$$f_{yT} = \left[1 + \frac{T}{900\ln(T/1750)}\right]\times f_y \qquad 0 < T \le 600^o C \tag{5a}$$

$$f_{yT} = \left[\frac{340 - 0.34T}{T - 240}\right]\times f_y \qquad T > 600^o C \tag{5b}$$

2.2.5 Young's modulus of steel

The model presented by Lie (1992) is used to predict young's modulus of steel at the elevated temperature (E_T):

$$E_T = \left[1 + \frac{T}{2000\times\ln\left(\frac{T}{1100}\right)}\right]\times E_s \qquad 0 < T \le 600^o C \tag{6a}$$

$$E_T = \left[\frac{690 - 0.69\times T}{T - 53.5}\right]\times E_s \qquad T > 600^o C \tag{6b}$$

2.3 Prediction of shear capacity

The MCFT was developed by Vecchio and Collins (1986) based on experimental observations of a large number of RC members. It uses equilibrium, compatibility and stress-strain relationships to predict the relationship between shear and normal stresses as well as the resulting deformations. The MCFT has been successfully implemented in a number of computer programs including Response 2000 (Bentz, 2000), which is utilized in this paper.

When a beam is exposed to fire from three sides, the pattern of temperature distribution within the beam cross-section takes the shape of the contour lines shown in Figure 3(a). This varying temperature within the beam cross-section poses a challenge while defining the temperature to be used to calculate the reduced strength properties of materials.

To utilize the method of sectional analysis during fire exposure, El-Fitiany and Youssef (2009) divided the concrete section into layers and assigned an average temperature to each layer, Figure 3(b). The same approach is valid while evaluating the shear behavior as the MCFT can be applied using a layered approach (Vecchio and Collins, 1988). A further simplification that involves the use of one average temperature for the whole section is examined by developing two models for six concrete sections. In the first model (Figure 4a), each section is assumed to have five layers with different temperatures assigned to each layer. The second model (Figure 4b) uses an average temperature for the whole section. Table 1 gives the details of the six analyzed sections. The shear capacities predicted by the two models are then evaluated using the MCFT. Figure 5 compares the shear capacities predicted by the two models, which have a maximum difference of 4%.

As the vertical legs of the stirrups provide shear resistance, their temperatures are used to

calculate the material properties. Temperatures at mesh points that lie on the vertical legs were obtained from the heat transfer analysis. The average of these temperatures is then calculated. The use of such average is justified because the distance between the mesh points are equal and shear stresses are assumed to be constant along the stirrup height. The average temperature was then utilized to calculate the reduced strength properties of the shear reinforcement.

3. Validation of the proposed method

The proposed method to estimate the shear capacity of RC beams during exposure to fire is validated by comparing its predictions with the experimental and analytical data found in the literature. It has been quite difficult, however, to find literature discussing the shear resistance of RC beams exposed to fire. The majority of the research on fire resistance of concrete structural elements has mainly been conducted to study flexural resistance rather than shear resistance.

3.1 Experimental work by Desai et al. (1998)

Desai (1998) tested five RC beams that were exposed to fire from three sides to evaluate their shear capacity. All beams were $200 \times 300\ mm$ in cross-section. They had $1600\ mm$ overall length and $1400\ mm$ supported span. The beams were reinforced using $3\varphi 20\ mm$ and $2\varphi 12\ mm$ at their bottom and top, respectively. Concrete cover was $25\ mm$. Table 2 gives details about the stirrups and the concrete compressive strength for the tested beams. Figure 6 shows the cross-section of beam B501. Desai (1998) proposed the use of a center bar to enhance the fire resistance. The tensile strength of the steel reinforcement at ambient temperature (f_y) was $460\ MPa$. Beams B102, B202, B301, B401 and B501 were exposed to ISO 840 fire curve while supporting a midspan load of 70,

80, 90, 110, and 120 kN, respectively. The fire durations resulting in shear failure were recorded. Analysis steps for beam B501 are given as an example of the application of the proposed method.

3.1.1 Temperatures in concrete and steel during exposure to fire

Heat transfer analysis was performed to determine the temperature distribution within the cross-section of the beam. The section was divided into 45^o mesh elements and the temperature for each element was obtained. The cross-section was then divided into 120 layers and the average temperature for each layer is calculated. Figure 7 shows the variation of average temperatures for the whole section at different fire durations. The average temperature in concrete reached 617 ℃ after approximately two hours of fire exposure.

Figure 8 shows the increase in temperatures in the steel bars during the fire event. Locations of steel bars are identified in Figure 6. The temperatures of bars located at L_1, L_2, L_3, and L_4 reached 643, 565, 370, and 460 ℃, respectively, after two hours of fire exposure. It can be seen that bars L_1 and L_2 experienced a higher temperature increase as they are located close to the fire-exposed faces of the beam. On the other hand, bar L_3 (the center bar) experienced the lowest temperature increase. Temperatures resulting from heat transfer analysis were recorded along the vertical leg of the stirrups at 4 mm spacing. The average temperature within the leg was then calculated. Figure 8 shows that the average temperature in stirrups reached 640 ℃ after two hours of fire exposure.

3.1.2 Properties of materials during fire

The strength properties for steel and concrete during fire exposure are shown in Figure 9 to Figure 12. The stirrups and the tension steel bars, located at the bottom side of the beam, experienced high reduction in strength properties as shown in Figure 9 and Figure 10. Figure 9

shows that the yield strength of the stirrups decreased by 70% after two hours of fire exposure as compared to only 26% decrease for the center bar. Young's modulus of the stirrups decreased by 59% after two hours of fire exposure as compared to a decrease of only 17% for the center bar as shown in Figure 10. The concrete compressive strength decreased by 69% after two hours of fire exposure, Figure 11. The reduction in the concrete tensile strength is shown in Figure 12.

3.1.3 Reduction of shear capacity during fire exposure

Figure 13 shows the reduction of the shear capacity of beam B501 during exposure to a fire as predicted by the MCFT. The beam failed in shear after $1.72\ hrs$ of fire exposure as its shear capacity was reduced to 42% of its initial shear capacity. Desai et al. (1998) reported that the beam failed after $1.78\ hr$ of fire exposure.

3.1.4 Shear capacity predictions for the remaining beams

Figure 14 shows the reduction in the shear capacities of beams B102, B202, B301, B401 and B501. Desai et al. (1998) reported that beams B102, B202, B301, B401 and B501 failed after $1.88, 1.68, 1.70, 1.76, and\ 1.78\ hrs$ of fire exposure, respectively. For the same shear forces, the proposed method predicted the beams to fail after $1.77, 1.55, 1.56, 1.75$ and $1.72\ hr$s of fire exposure. Figure 15 presents a comparison between the predictions of the proposed method and the experimental results for all beams. It is clear that the proposed method predicted with sufficient accuracy the shear capacity of fire-exposed beams during exposure to a fire.

3.2 Hsu and Lin's analytical work

Hsu and Lin (2008) developed an analytical model that incorporates thermal and structural

analyses to assess the shear capacity of RC beams during fire exposure. They used the finite difference method to model the temperature distribution within the cross-section. The shear capacity was then evaluated using the equation of the American Concrete Institute design standard (ACI, 2008) while considering the influence of elevated temperatures on the properties of steel and concrete. They analyzed a beam that had 300×500 mm cross-section. It was reinforced with $4\varphi 25\ mm$ at its bottom and $2\varphi 25\ mm$ at its top. Stirrups of $\varphi 10\ mm$ spaced at $100\ mm$ were used. The ambient compressive strength of concrete was $20\ MPa$ and the ambient yield strength of the steel bars was $400\ MPa$. The proposed method is applied to the same beam. Figure 16 shows a good match between the prediction of the proposed method and results by Hsu and Lin (2008).

4. Parametric study

A total of 26 beams were analyzed, Table 3. Three beam heights (300 , 400 and $500\ mm$), three beam widths ($200, 300$ and $400\ mm$), two longitudinal reinforcements ratios (1.5% and 2.5%), four transverse reinforcement ratios ($0.0\%, 0.2\%, 0.4\%$ and 0.6%), two concrete covers (30 and $40\ mm$), and two concrete compressive strengths (30 and $50\ MPa$) were considered. These beams were subjected to fire from three sides. Fire temperatures were based on the standard ISO 840 fire curve (Lie, 1992). The following sections provide a detailed analysis of the effect of each parameter considered in this study.

4.1 Effect of the transverse reinforcement ratio (ρ_t)

Figure 17 tacks the shear capacity reduction, during exposure to elevated temperatures for beams with different percentage of transverse reinforcement. Figure 18 shows the relationship between the percentage of transverse reinforcement and the shear capacity at different durations of fire exposure.

The reductions in the shear capacity after 1 hr and 2 hr of fire exposure are 22% and 57% for B2, and 26% and 60% for B4. These numbers suggest that the reduction rate of the shear capacity during fire is not significantly affected by the transverse reinforcement ratio. By increasing the transverse reinforcement ratio (ρ_t) from 0.2% to 0.4%, the shear capacity increased by 49% at ambient temperature, and by 40% and 37% after 1 hr and 2 hr of fire exposure, respectively. Similarly, by increasing the transverse reinforcement ratio (ρ_t) from 0.4% to 0.6%, the shear capacity is increased by 27% at ambient temperature, and by 24% and 20% after 1 hr and 2 hr of fire exposure, respectively. It can be noted that the benefit of using additional shear reinforcement decreases during fire because of the reduction of the steel strength properties.

4.2 Effect of the longitudinal reinforcement ratio (ρ_l)

Figure 19 tracks the shear capacity reduction, during exposure to elevated temperatures, of four beams B2, B4, B5 and B7 that have the same cross-section dimensions. Beams B2 & B5 have same web reinforcement (0.2%), and two different percentages of longitudinal reinforcement (1.5% and 2.5%). Beams B4 and B7 have same web reinforcement (0.6%) and two different percentages of longitudinal reinforcement (1.5% and 2.5%).

a) Beams with 0.2% transverse reinforcement:

   The shear capacity of beam B2, which has longitudinal reinforcement of 1.5%, is reduced by 22% and 57% after 1 hr and 2 hr of fire exposure, respectively. The shear capacity of beam B5, which has a longitudinal reinforcement of 2.5%, is reduced by 20% and 55% after 1 hr and 2 hr of fire exposure, respectively.

b) Beams with 0.6% transverse reinforcement:

   The shear capacity of beam B4, which has a longitudinal reinforcement of 1.5%, is reduced by

26% and 60% after 1 hr and 2 hr of fire exposure, respectively. The shear capacity of beam B7, which has a longitudinal reinforcement of 2.5%, is reduced by 24% and 59% after 1 hr and 2 hr of fire exposure, respectively.

Increasing the percentage of longitudinal reinforcement slightly increases the shear capacity of beams. However, it does not affect the shear capacity reduction rate during exposure to fire.

4.3 Effect of concrete cover

Figure 20 tracks shear capacity reduction, during exposure to elevated temperatures, of beams B2, B4, B8, and B10. Beams B2 & B4 have a 30 mm concrete cover, while beams B8 & B10 have a 40 mm concrete cover.

a) Beams with 0.2% transverse reinforcement:

   The shear capacity of beam B2, which has a 30 mm concrete cover, is reduced by 22% and 57% after 1 hr and 2 hr of fire exposure, respectively. On the other hand, the shear capacity of beam B8, which has a 40 mm concrete cover, is reduced by 14% and 44% after 1 hr and 2 hr of fire exposure, respectively.

b) Beams with 0.6% transverse reinforcement:

   The shear capacity of beam B4, which has a 30 mm concrete cover, is reduced by 26% and 60% after 1 hr and 2 hr of fire exposure, respectively. On the other hand, the shear capacity of beam B10, which has a 40 mm concrete cover, is reduced by 20% and 50% after 1 hr and 2 hr of fire exposure, respectively. Increasing the concrete cover from 30 mm to 40 mm increased the shear capacity by 8% and 24% after 1 hr and 2 hr of fire exposure, respectively.

4.4 Effect of beam height (h)

Figure 21 tracks the shear capacity reduction during exposure to elevated temperatures for beams B1, B3, B11, B13, B21 and B23. Beams B1 and B3 have a 300 mm beam height and web reinforcement percentages of 0% and 0.4%, respectively. Beams B11 and B13 have a 400 mm beam height and web reinforcement percentages of 0% and 0.4%, respectively. Beams B21 and B23 have a 500 mm beam height and web reinforcement percentages of 0% and 0.4%, respectively.

a) Beams with no transverse reinforcement:

   The shear capacity of beam B1, which has a 300 mm beam height, is reduced by 25% and 64% after 1 hr and 2 hr of fire exposure, respectively. The shear capacity of beam B11, which has a 400 mm beam height, is reduced by 20% and 52% after 1 hr and 2 hr of fire exposure, respectively. The shear capacity of beam B21, which has a 500 mm beam height, is reduced by 18% and 48% after 1 hr and 2 hr of fire exposure, respectively.

b) Beams with 0.4% transverse reinforcement:

   The shear capacity of beam B3, which has a 300 mm beam height, is reduced by 26% and 59% after 1 hr and 2 hr of fire exposure, respectively. The shear capacity of beam B13, which has a 400 mm beam height, is reduced by 24% and 58% after 1 hr and 2 hr of fire exposure, respectively. The shear capacity of beam B23, which has a 500 mm beam height, is reduced by 22% and 56% after 1 hr and 2 hr of fire exposure, respectively.

Increasing the beam height results in a higher shear capacity. The reduction rate of this capacity during exposure to a fire event is not affected by increasing the beam height for beams with web reinforcement. This is due to the fact that increasing the beam height has a minor effect on the temperature of the web reinforcement.

4.5 Effect of beam width (b)

Figure 22 tacks the shear capacity reduction, during exposure to elevated temperatures, of four beams B21, B23, B24 and B26. Beams B21 and B24 have no transverse reinforcement and two different widths $200\ mm$ and $400\ mm$, respectively. Beams B23 and B26 have 0.4% transverse reinforcement and two different widths $200\ mm$ and $400\ mm$, respectively.

a) Beams with no transverse reinforcement:

   The shear capacity of beam B21, which has a $200\ mm$ beam width, is reduced by 18% and 48% after $1\ hr$ and $2\ hr$ of fire exposure, respectively. On the other hand, the shear capacity of beam B24, which has a $400\ mm$ beam width, is reduced by 8% and 16% after $1\ hr$ and $2\ hr$ of fire exposure, respectively.

b) Beams with 0.4% transverse reinforcement:

   The shear capacity of beam B23, which has a $200\ mm$ beam width, is reduced by 23% and 56% after $1\ hr$ and $2\ hr$ of fire exposure, respectively. On the other hand, the shear capacity of beam B26, which has a $400\ mm$ beam width, is reduced by 18% and 39% after $1\ hr$ and $2\ hr$ of fire exposure, respectively.

It can be seen that beams with larger width are less affected by fire hazards. Increasing the beam width is an effective way to maintain the shear capacity during fire as the concrete core is protected from fire temperature. Beams with large width and transverse reinforcement experienced higher reduction rates of shear capacity than beams with no transverse reinforcement. This is due to the fact that temperature of web reinforcement is not affected by the beam width.

4.6 Effect of concrete compressive strength (f'_c)

Figure 23 tracks the shear capacity reduction, during exposure to elevated temperatures, of

beams B1, B3, B4, B17, B19 and B20. To investigate the effect of concrete compressive strength (f'_c), the beams are divided into two groups: beams B1, B3 and B4 have a concrete compressive strength of $30\ MPa$, while beams B17, B19 and B20 have a concrete compressive strength of $50\ MPa$. Beams (B1 & B17), (B3 & B19) and (B4 & B20) have web reinforcement percentages of 0.0%, 0.4% and 0.6%, respectively.

a) Beams with no transverse reinforcement:

   The shear capacity of beam B1, which has a $30\ MPa$ compressive strength, is reduced by 25% and 64% after $1\ hr$ and $2\ hr$ of fire exposure, respectively. On the other hand, the shear capacity of beam B17, which has a $50\ MPa$ compressive strength, is reduced by 23% and 57% after $1\ hr$ and $2\ hr$ of fire exposure, respectively.

b) Beams with 0.6% transverse reinforcement:

   The shear capacity of beam B4, which has a $30\ MPa$ compressive strength, is reduced by 26% and 60% after $1\ hr$ and $2\ hr$ of fire exposure, respectively. On the other hand, the shear capacity of beam B20, which has a $50\ MPa$ compressive strength, is reduced by 27% and 63% after $1\ hr$ and $2\ hr$ of fire exposure, respectively.

Using higher compressive strength (f'_c) slightly increases the shear capacity of the beam. The effect of using higher concrete compressive strength becomes less pronounced for longer fire durations for beams with web reinforcement. This is due to the fact that web reinforcement has a greater contribution to the beam shear capacity and at high temperatures the effect of the deterioration of web reinforcement overcomes the deterioration of concrete strength.

5. Summary and conclusions

An analytical method to predict the shear capacity of RC beams exposed to elevated

temperatures is proposed. The proposed method extends the use of existing ambient temperature methods while accounting for the effect of elevated temperatures on the materials. The finite difference method is implemented to perform a heat transfer analysis. The deteriorated concrete and steel strength properties are then calculated based on the elevated temperatures. Shear capacity was subsequently estimated using the modified compression field theory. The predictions of the proposed method were found to have a good agreement with the experimental and analytical results found in the literature. Additional research is needed to further improve the proposed method to account for concrete spalling, and, thus be valid for high strength concrete.

A parametric study was then conducted to investigate the effects of different parameters on the shear capacity of RC beams exposed to fire. The parametric study provided data about the sensitivity of shear capacity to different parameters and confirmed the relative importance of each parameter.

References

ACI (2008) *Building code requirements for structural concrete (ACI 318-08) and commentary*, American Concrete Institute, Framinton Hills, MI, USA.

BAMONTE, P, FELICETTI, R and GAMBAROVA, P (2009) Punching Shear in Fire-Damaged Reinforced Concrete Slabs. *ACI Special Publication,* 265**,** 345-366.

BENTZ, EC (2000) *Sectional analysis of reinforced concrete members.* PhD Thesis, Department of Civil Engineering, University of Toronto, Ontario, Canada.

DENOËL, JF (2007) *Fire safety and concrete structures,* Federation of Belgian Cement Industry, FEBELCEM, Brussels, Belgium.

DESAI, SB (1998) Design of reinforced concrete beams under fire exposure conditions. *Magazine of Concrete Research,* 50(1)**,** 75-83.

EL-FITIANY, S and YOUSSEF, MA (2009) Assessing the flexural and axial behaviour of reinforced concrete members at elevated temperatures using sectional analysis. *Fire Safety Journal,* 44(5)**,** 691-703.

EL-FITIANY, S and YOUSSEF, MA (2010) A simplified sectional analysis approach for RC elements during fire events. 6th International Conference on Structures in Fire, Michigan State University, East Lansing, MI, USA. 239-246.

EL-FITIANY, S and YOUSSEF, MA (2011) Stress-Block Parameters for Reinforced Concrete Beams During Fire Events. *ACI Special Publication,* 279**,** 1-39.

EL-FITIANY, S and YOUSSEF, MA (2014a) Simplified Method to Analyze Continuous Reinforced Concrete Beams during Fire Exposure. *ACI Structural Journal,* 111**,** 145-156.

EL-FITIANY, S and YOUSSEF, MA (2014b) Interaction diagrams for fire-exposed reinforced concrete sections. *Engineering Structures,* 70**,** 246-259.

HERTZ, KD (2005) Concrete strength for fire safety design. *Magazine of Concrete Research,* 57(8)**,** 445-453.

HSU, J and LIN, C (2008) Effect of fire on the residual mechanical properties and structural performance of reinforced concrete beams. *Journal of Fire Protection Engineering,* 18(4)**,** 245-274.

KODUR, V, WANG, T and CHENG, F (2004) Predicting the fire resistance behaviour of high strength concrete columns. *Cement and Concrete Composites,* 26(2)**,** 141-153.

KOTSOVOS, GM and KOTSOVOS, MD (2013) Effect of axial compression on shear capacity of linear RC members without transverse reinforcement. *Magazine of Concrete Research,* 65(22)**,** 1360-1375.

LIE, TT (1992) *ASCE manuals and reports on engineering practice No. 78, structural fire protection,* American Society of Civil Engineers, New York, NY, USA.

MSAAD, Y and CHEFDEBIEN, A (2007) Temperature and shear capacity calculation for prestressed hollow core slabs under fire conditions. international workshop on Fire Design of Concrete Structures-from materials modelling to structural performance, University of Coimbra, Portugal. 351-357.

MURTY, DSRC and PAPARAO, G (2013) Influence of stirrup spacing on shear resistance of reinforced concrete beams. *Magazine of Concrete Research,* 65(14)**,** 829-836.

PURKISS, JA (2007) *Fire safety engineering design of structures*, Second Edition, Butterworth-Heinemann, Elsevier.

TERRO, MJ (1998) Numerical modeling of the behavior of concrete structures in fire. *ACI Structural Journal,* 95(2)**,** 183-193.

VECCHIO, FJ and COLLINS, MP (1986) The modified compression-field theory for reinforced concrete elements subjected to shear. *ACI Journal*, 83(2), 219–231.

VECCHIO, FJ and COLLINS, MP (1988) Predicting the response of reinforced concrete beams subjected to shear using the modified compression field theory. *ACI Structural Journal,* 85(3)**,** 258–268.

YOUSSEF, MA, EL-FITIANY, S and ELFEKI, M (2008) Flexural Behavior of Protected Concrete Slabs after Fire Exposure. *ACI Special Publication,* 255**,** 47-74.

YOUSSEF, MA and MOFTAH, M (2007) General stress–strain relationship for concrete at elevated temperatures. *Engineering Structures,* 29(10)**,** 2618-2634.

List of Figures:

List of Tables:

Table 1 Details of the six concrete cross-sections used to assess the average temperature approach

Beam No.	Beam Dimensions & Stirrups (mm)	Model (1)				Model (2)	
		Layer No.	Layer height (mm)	Temp. (°C)	Shear Capacity (kN)	Average Temp. (°C)	Shear Capacity (kN)
1	200 x 300 φ6@200mm	1	150	358	87	420	85
		2	60	370			
		3	40	436			
		4	25	555			
		5	25	760			
2	200 x 300 no stirrups	1	150	358	48	420	50
		2	60	370			
		3	40	436			
		4	25	555			
		5	25	760			
3	200 x 400 φ6@200mm	1	200	355	118	404	121
		2	80	363			
		3	54	395			
		4	35	501			
		5	31	731			
4	200 x 400 no stirrups	1	200	355	65	404	63
		2	80	363			
		3	54	395			
		4	35	501			
		5	31	731			
5	200 x 500 φ9@200mm	1	250	350	194	391	190
		2	100	355			
		3	65	370			
		4	45	455			
		5	40	690			
6	200 x 500 no stirrups	1	250	350	84	391	81
		2	100	355			
		3	65	370			
		4	45	455			
		5	40	690			

Table 2 Details of beam specimens (Desai et al., 1998)

Beam No.	f_c' (MPa)	Center bar	Stirrups
B102	39.40	-	-
B202	34.40	1φ16 mm	-
B301	42.00	1φ20 mm	-
B401	42.00	-	φ6mm@200 mm
B501	38.50	1φ16 mm	φ6mm@200 mm

Table 3 Parametric study beams

Beam #	f_c' (MPa)	b (mm)	h (mm)	ρ_l (%)	ρ_t (%)	Cover (mm)
B1	30	200	300	1.50	0.00	30
B2					0.20	
B3					0.40	
B4					0.60	
B5				2.50	0.20	
B6					0.40	
B7					0.60	
B8				1.50	0.20	40
B9					0.40	
B10					0.60	
B11			400		0.00	30
B12					0.20	
B13					0.40	
B14		300			0.00	
B15					0.20	
B16					0.40	
B17	50	200	300		0.00	
B18					0.20	
B19					0.40	
B20					0.60	
B21	30		500		0.00	
B22					0.20	
B23					0.40	
B24		400			0.00	
B25					0.20	
B26					0.40	

Figure 1
Click here to download Figure: 01- Proposed Method to Predict shear capacity of a RC beam exposed to fire..tiff

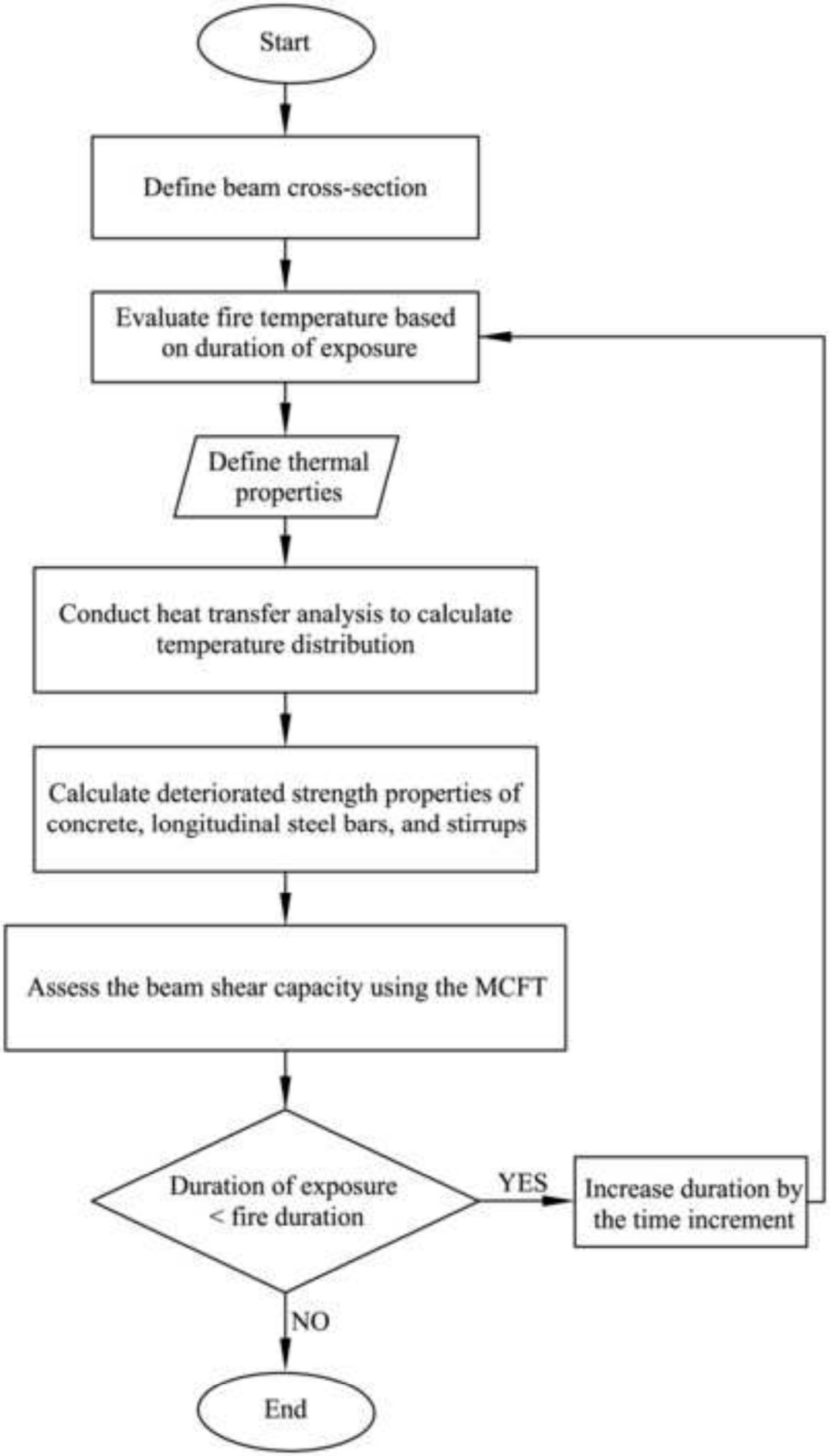

Figure 2
Click here to download Figure: 02- Typical heat transfer mesh.tiff

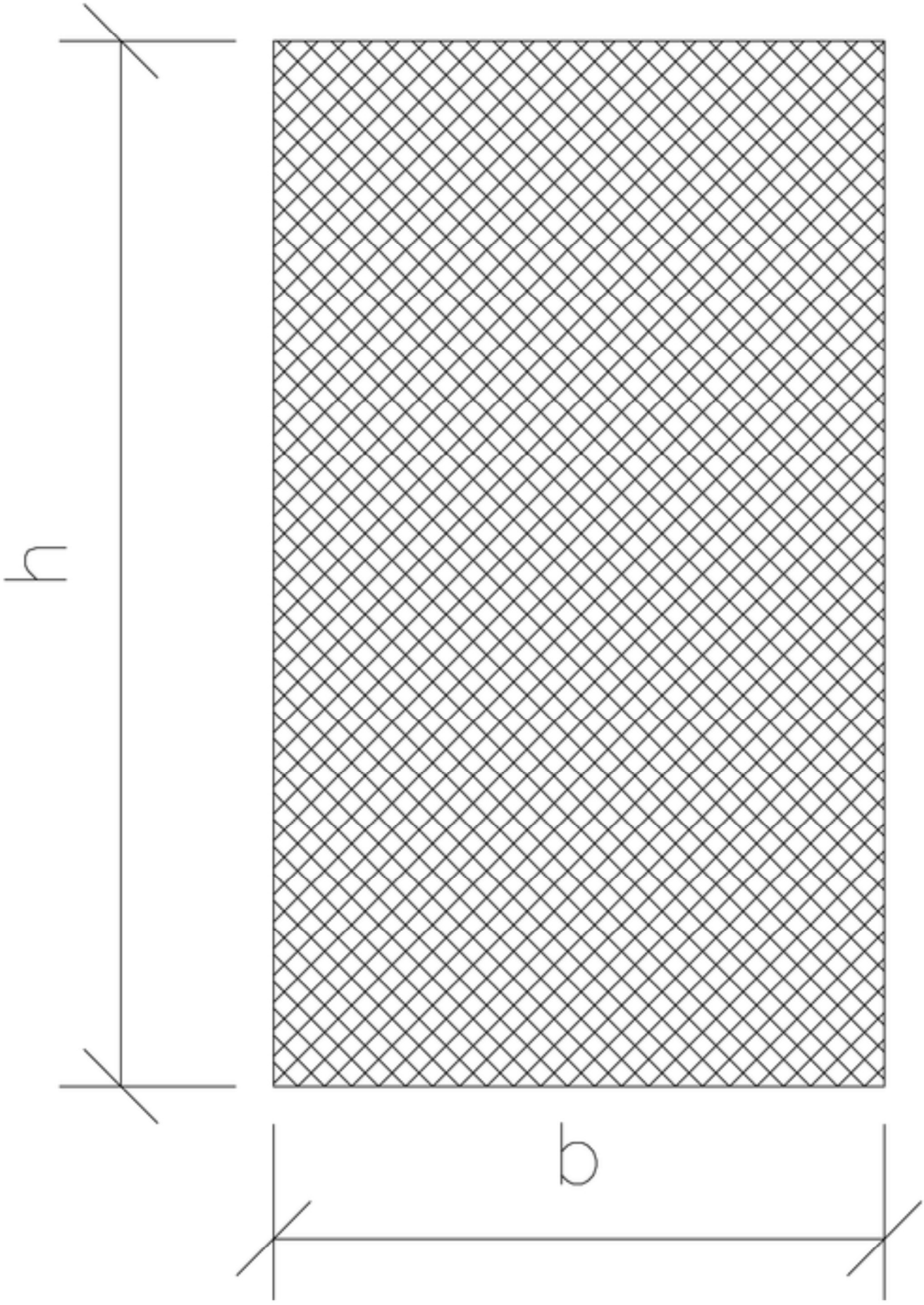

Figure 3a
Click here to download Figure: 03a-Contour lines.tiff

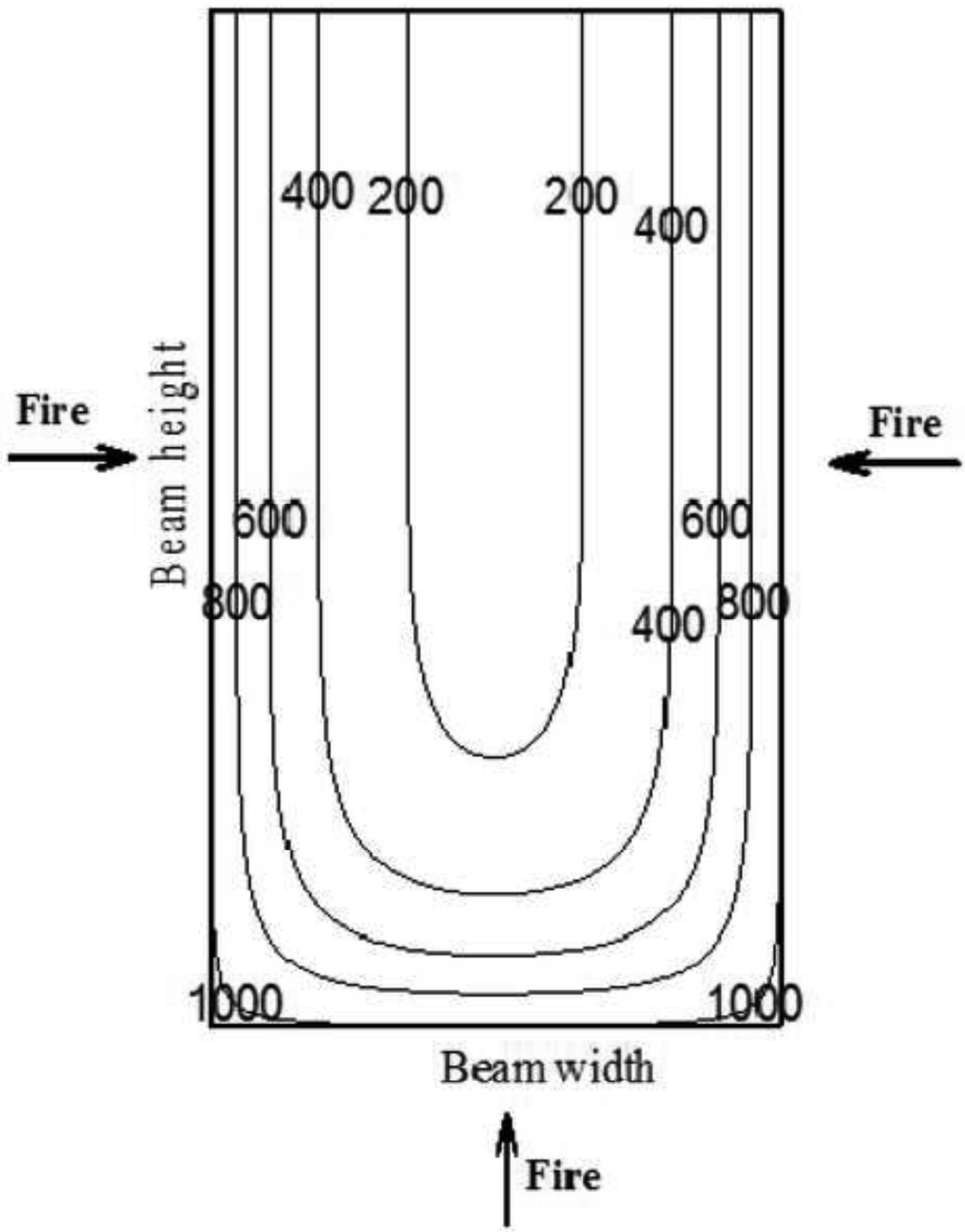

Figure 3b
Click here to download Figure: 03b-Concrete Layers.tiff

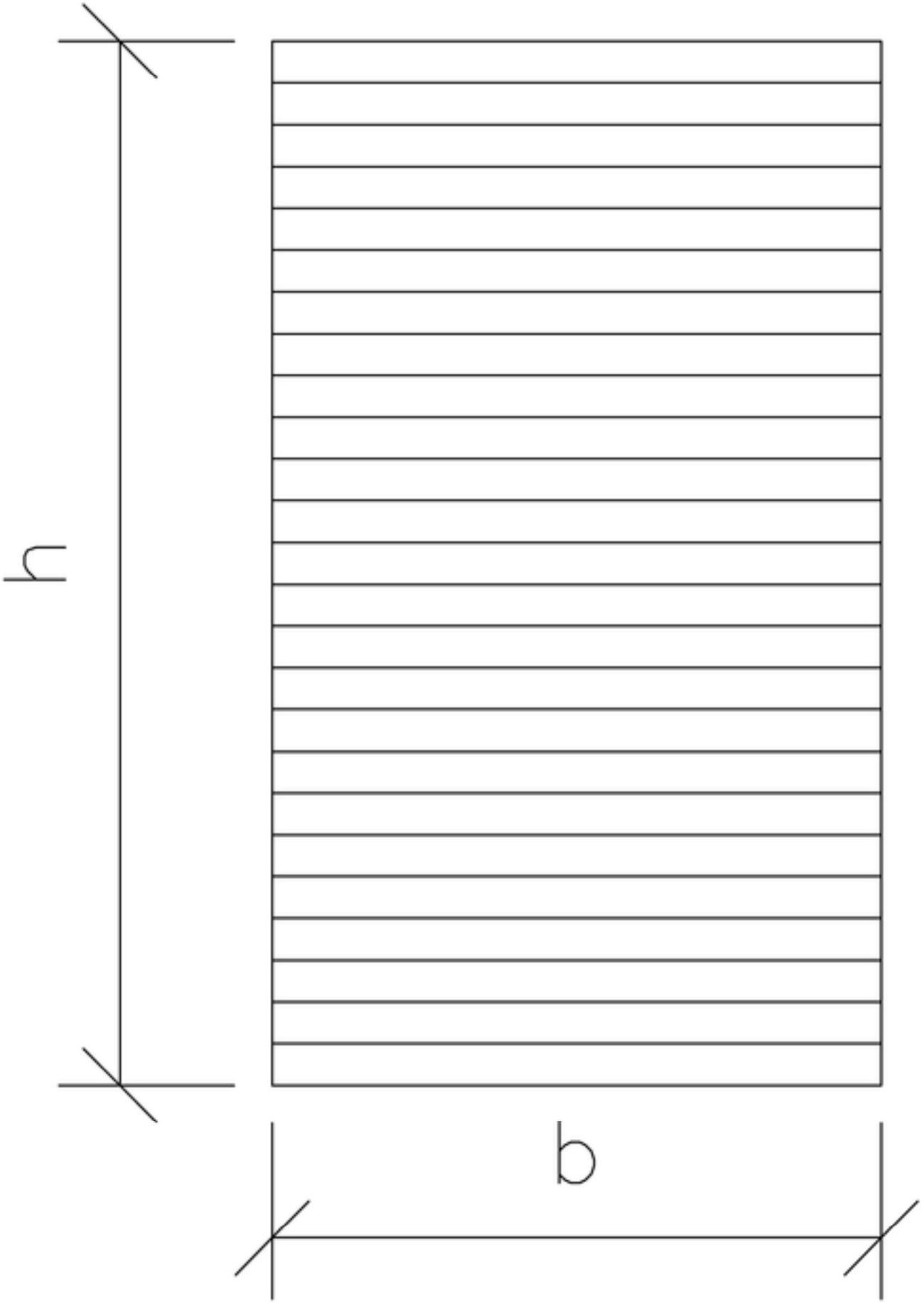

Figure 4
Click here to download Figure: 04- CUse of average temperature to evaluate the shear capacity. a-Model 1, b-Model 2.tiff

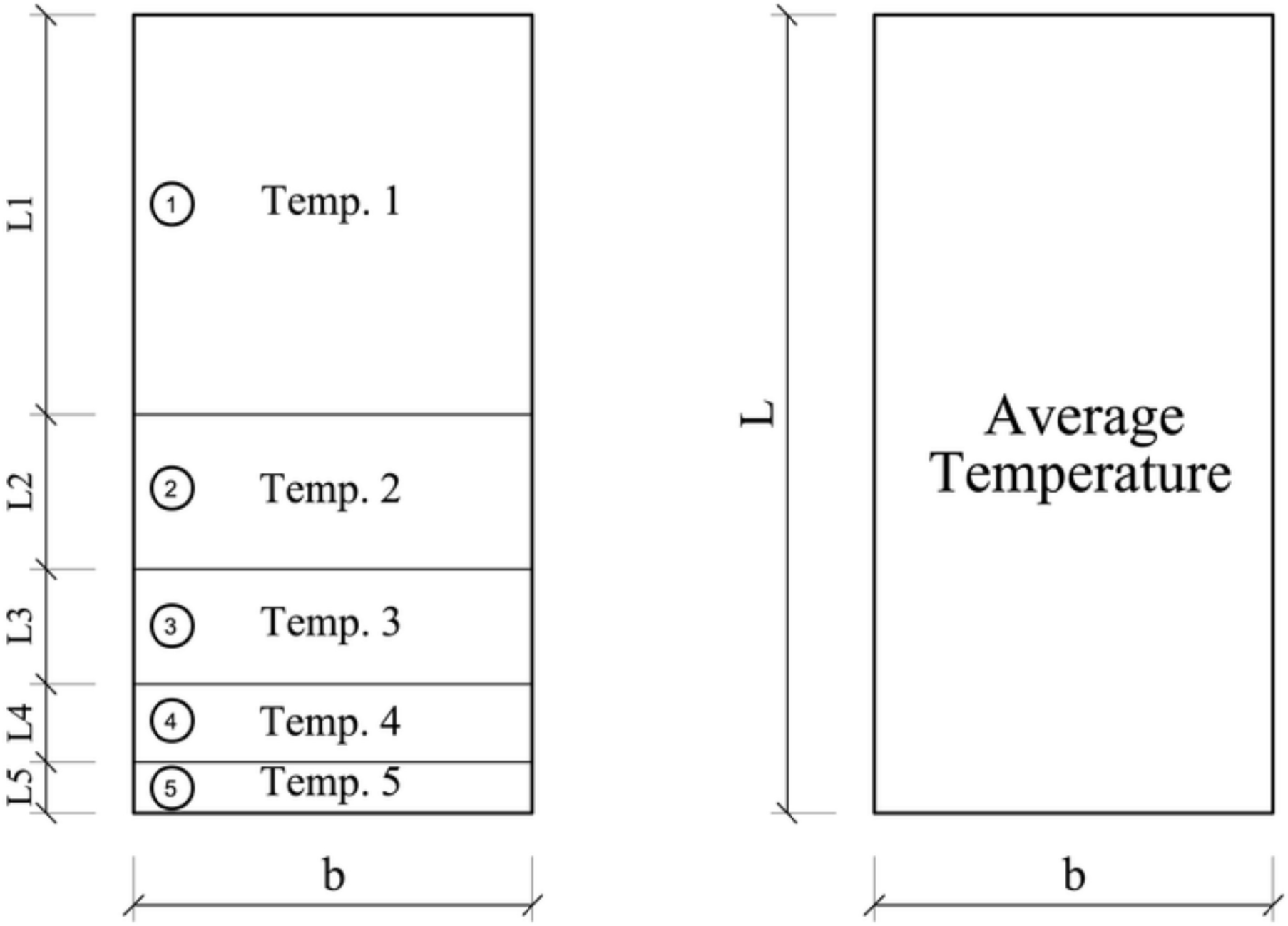

Figure 5
Click here to download Figure: 05- Effect of using an average concrete temperature on the shear capacity..tiff

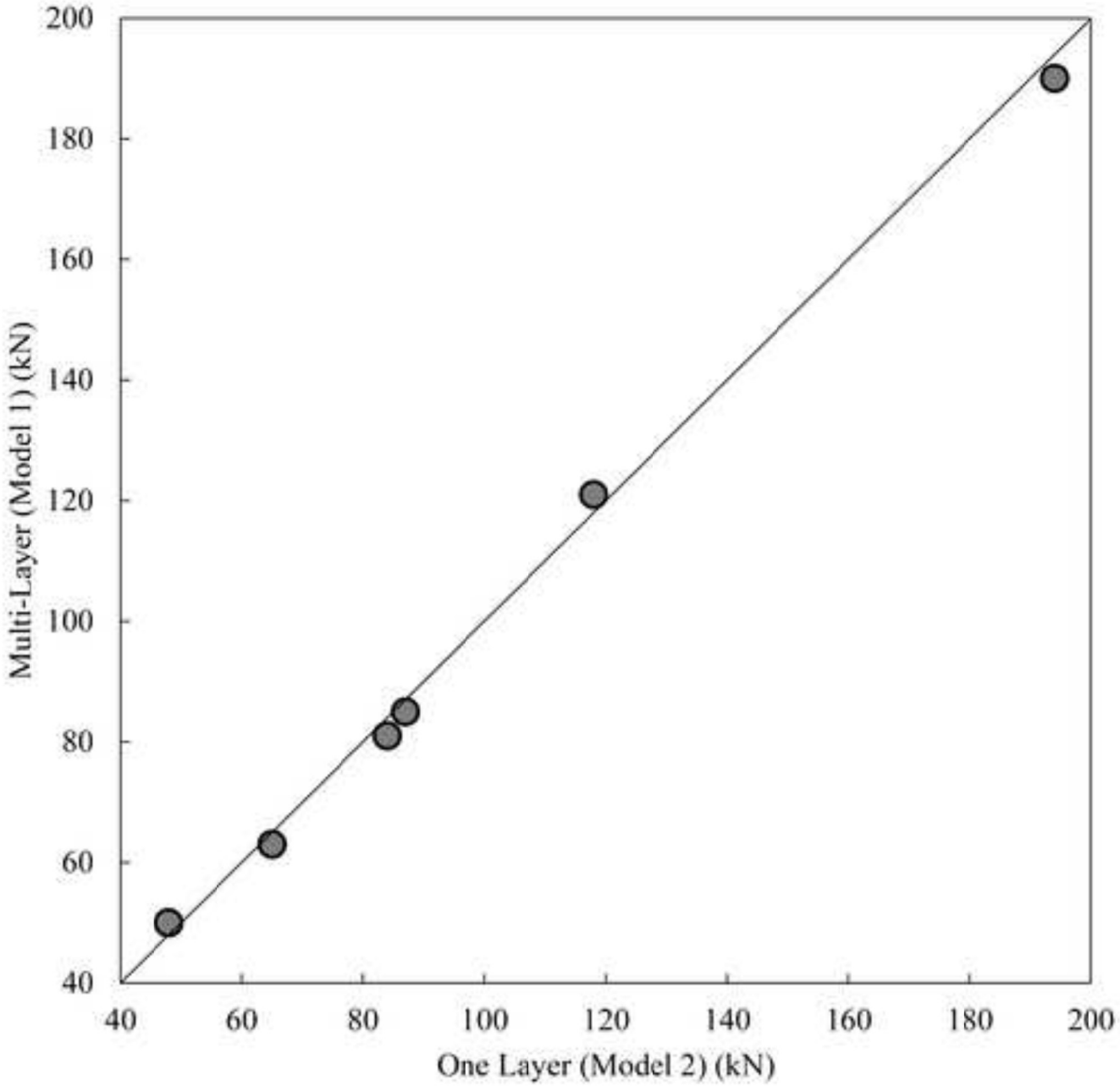

Figure 6
Click here to download Figure: 06-Cross-section of beam B501.tiff

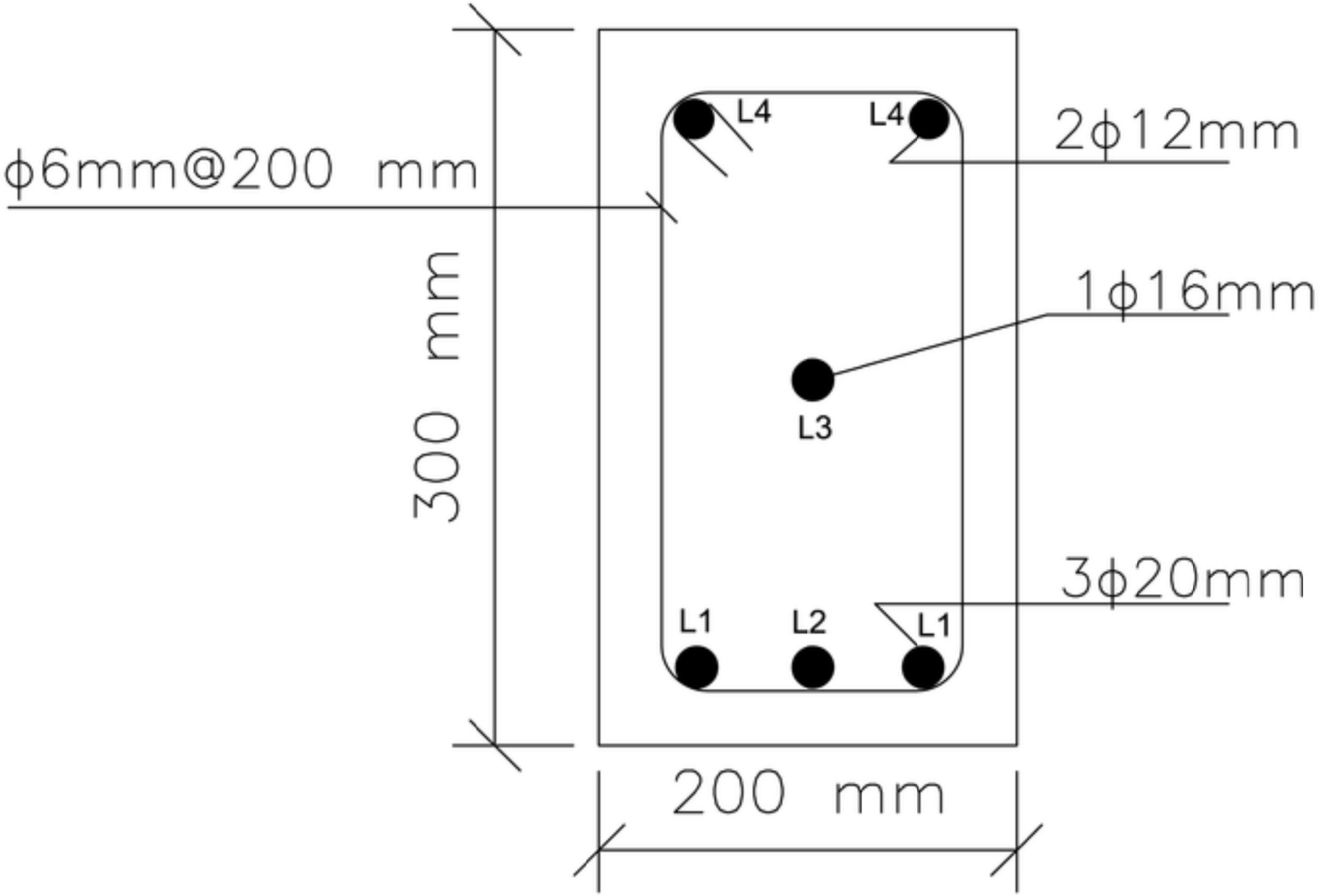

Figure 7
Click here to download Figure: 07- Average temperature in concrete during fire exposure..tiff

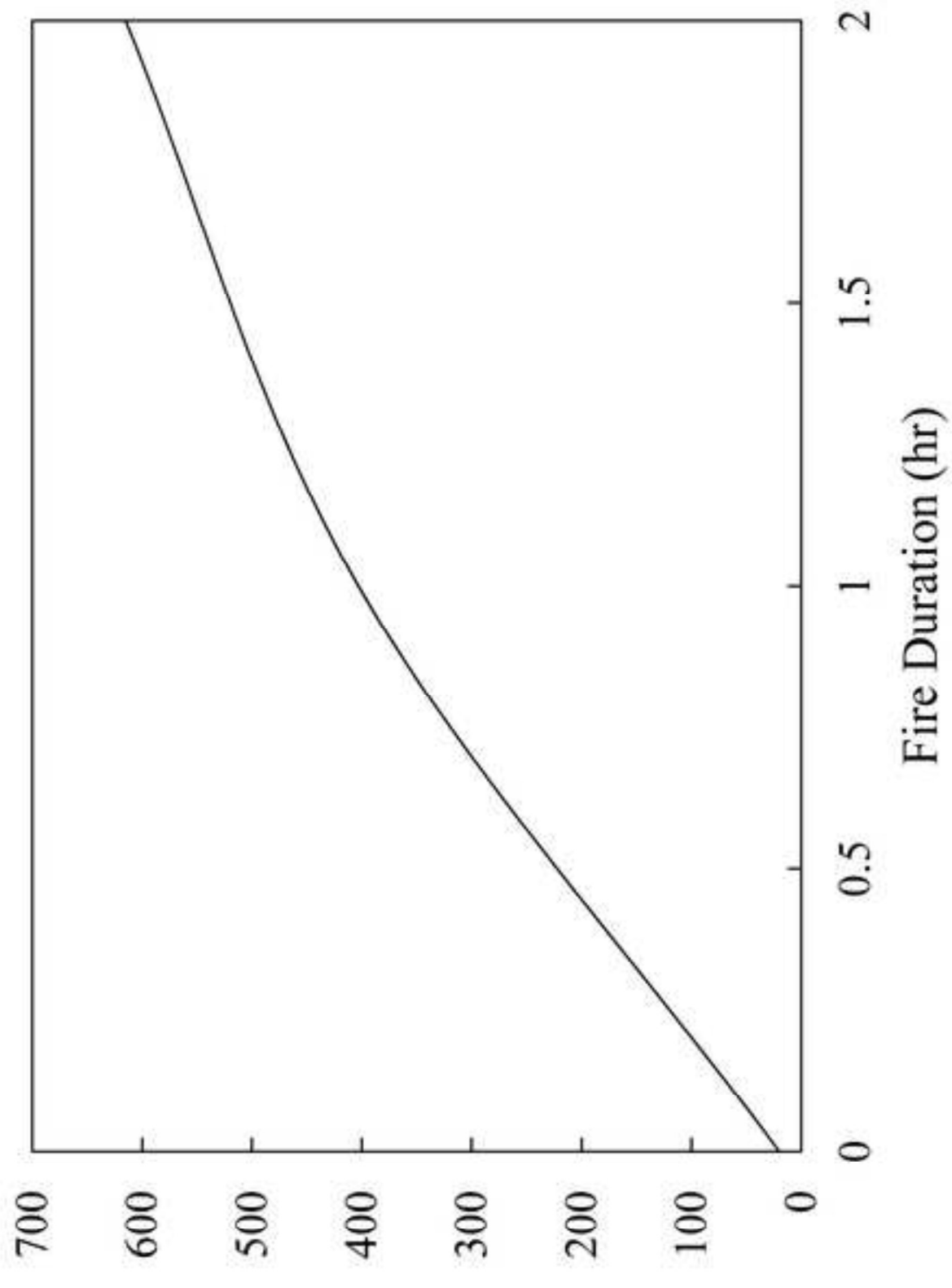

Figure 8
Click here to download Figure: 08- Temperatures in steel bars during fire exposure.tiff

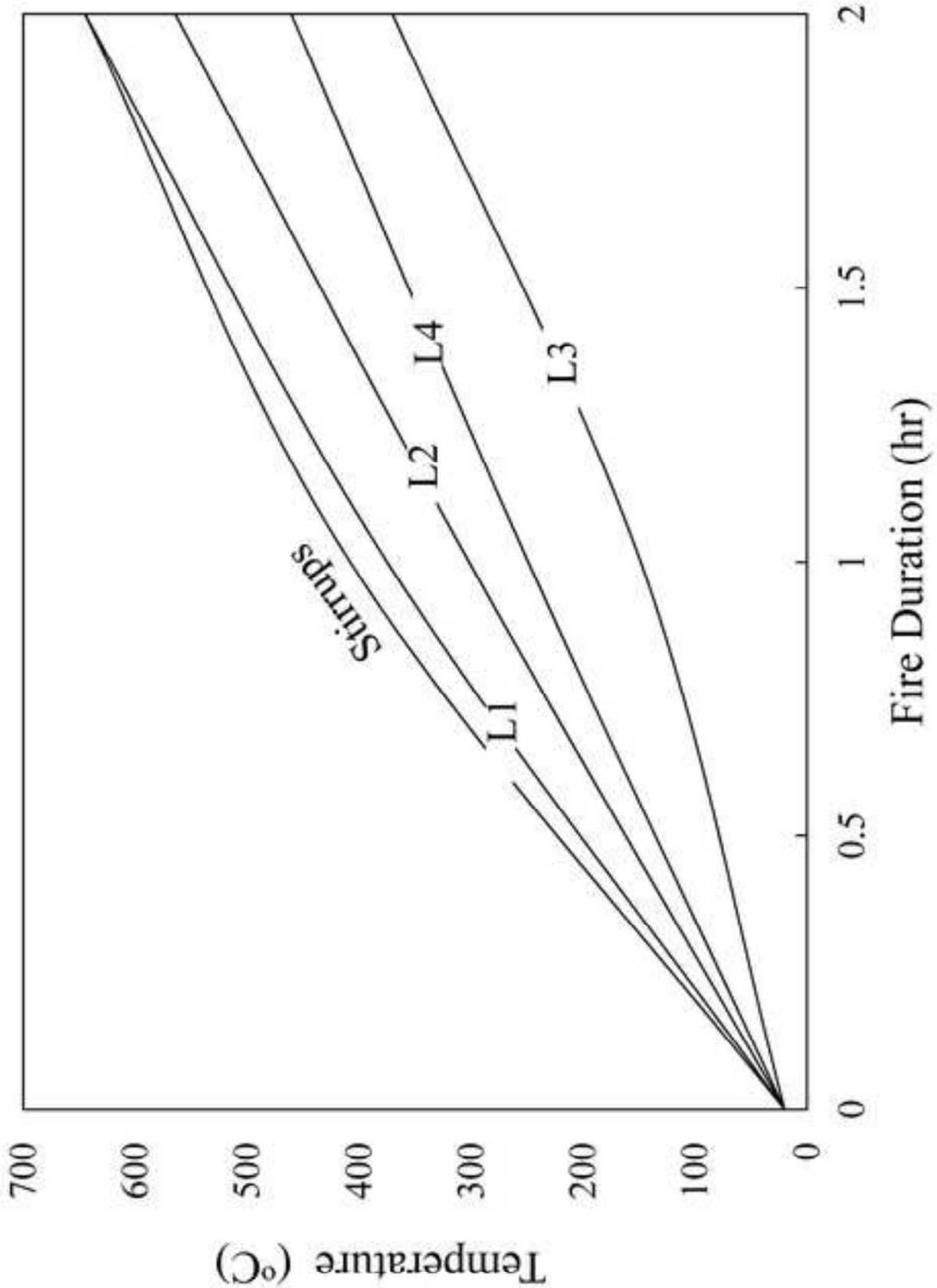

Figure 9
Click here to download Figure: 09- Reduction in yield strength of steel bars during fire exposure.tiff

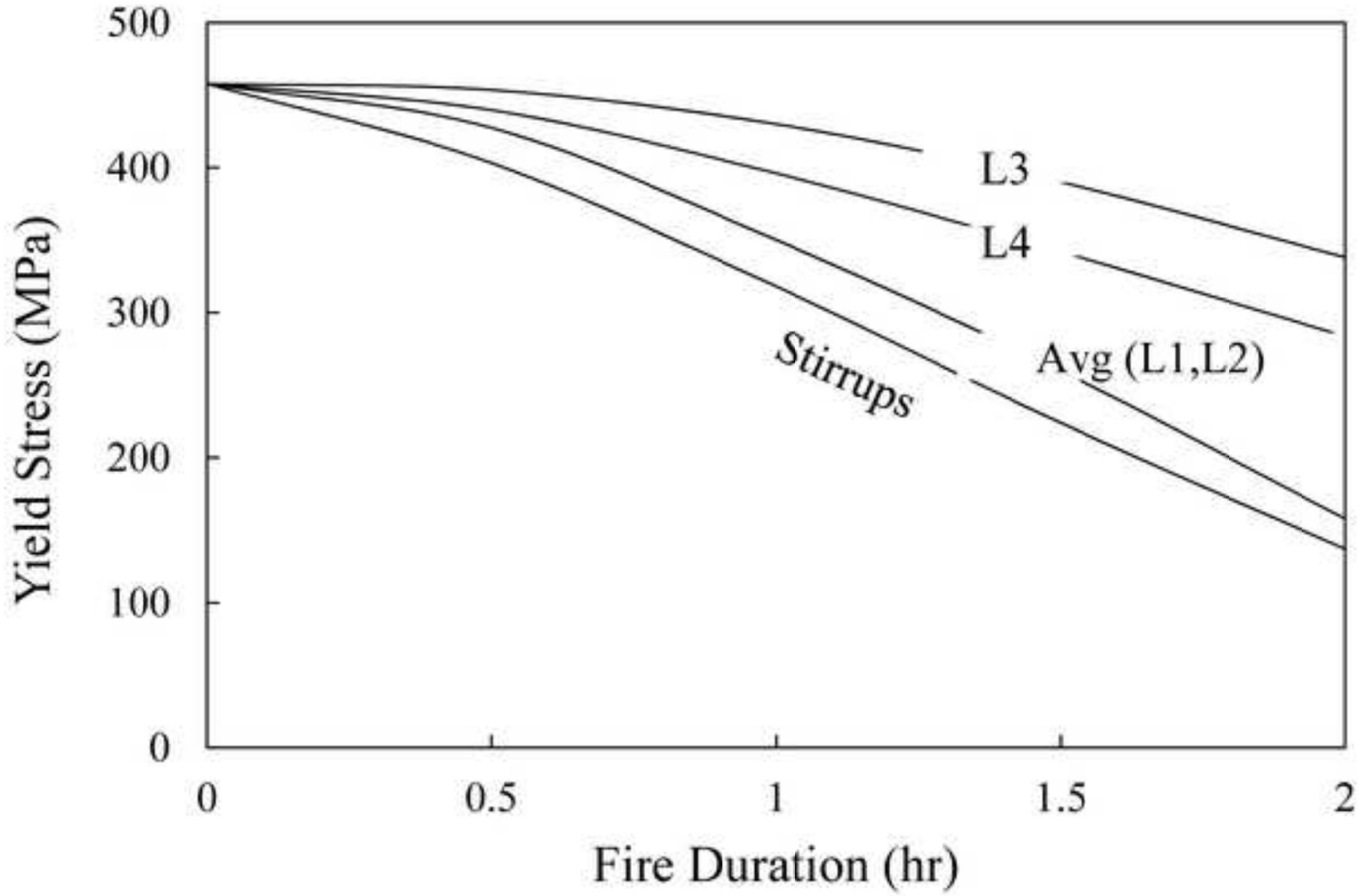

Figure 10
Click here to download Figure: renamed_415dd.tiff

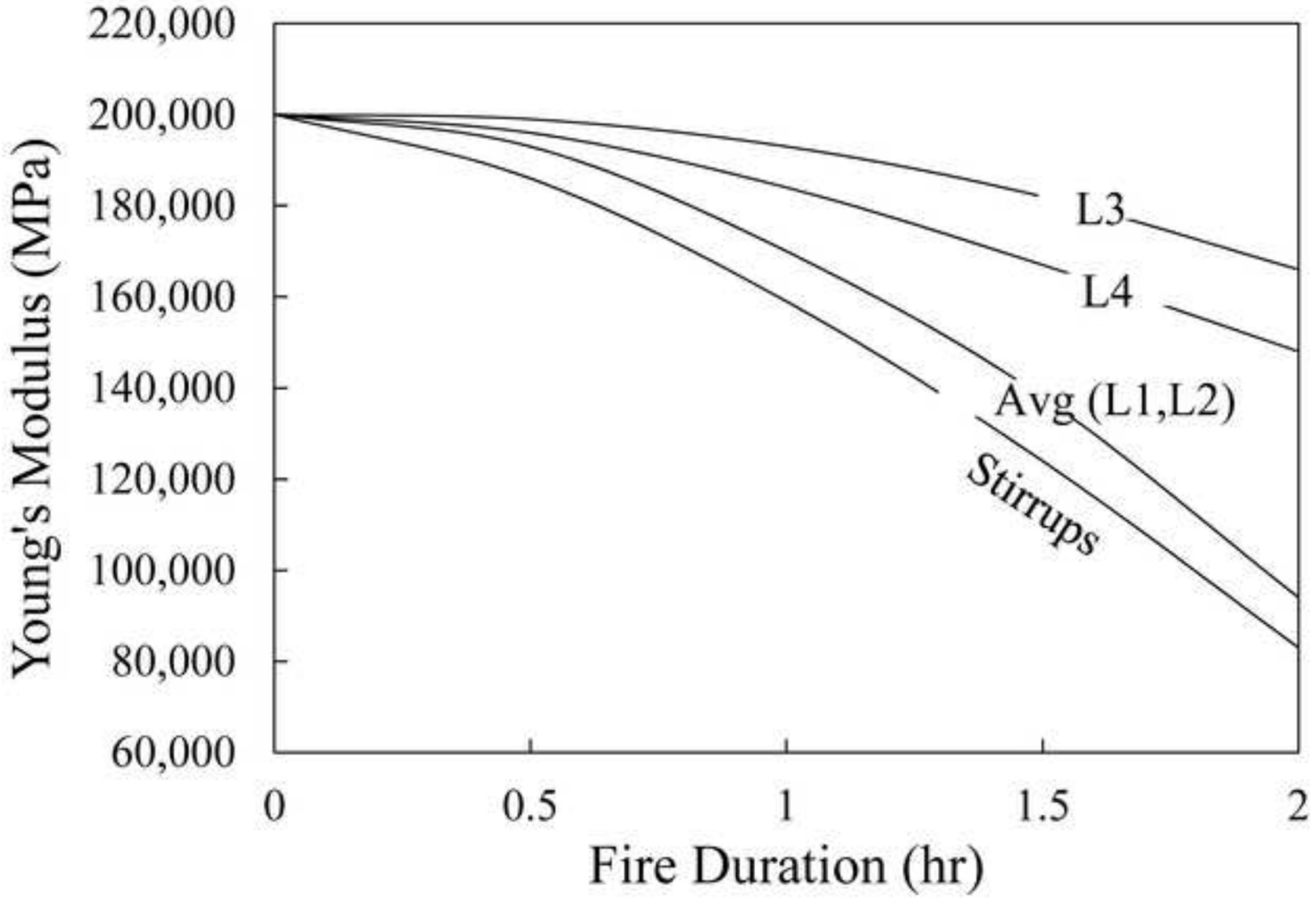

Figure 11
Click here to download Figure: 11- Reduction in concrete compressive strength during fire exposure..tiff

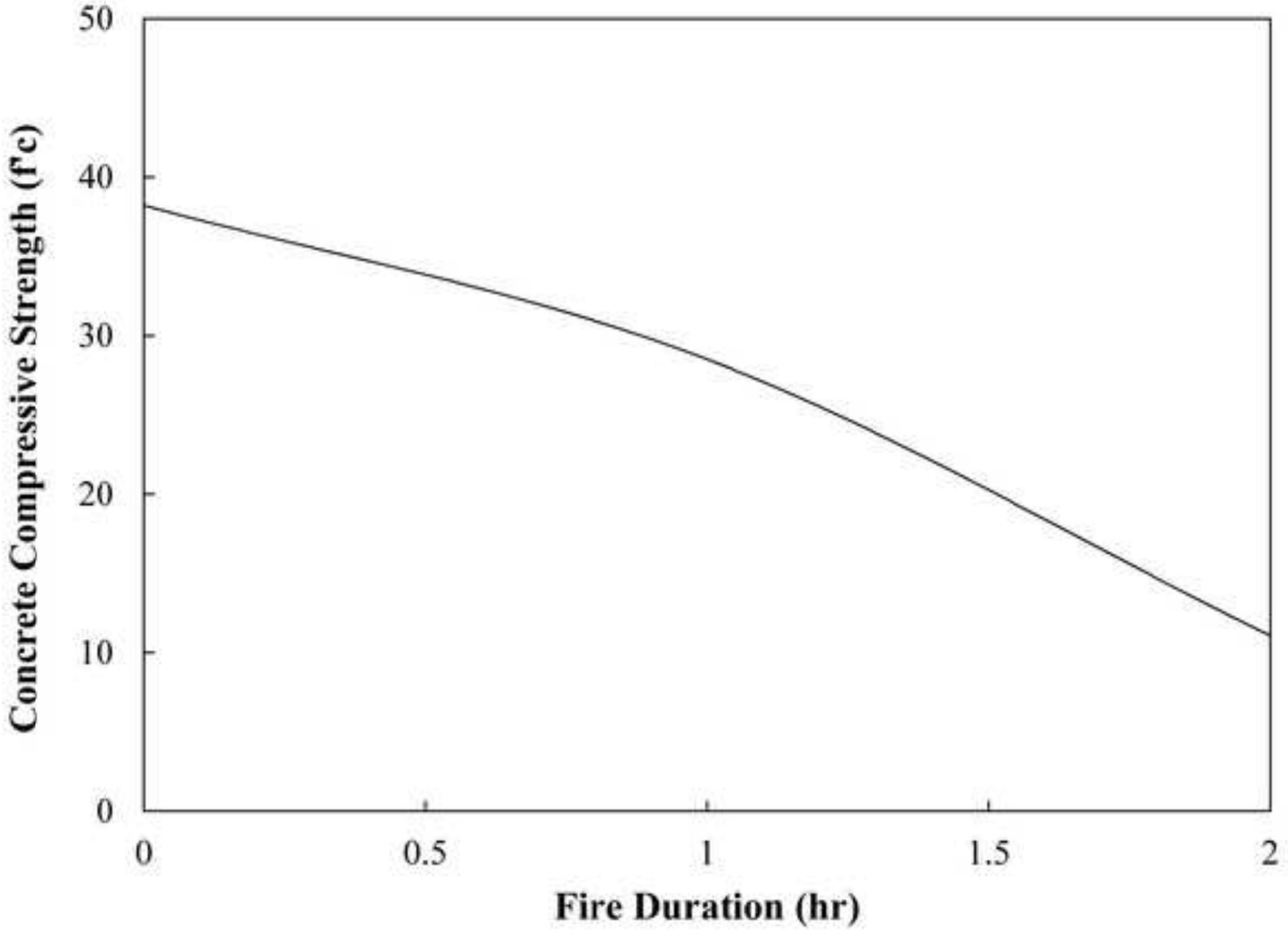

Figure 12
Click here to download Figure: 12- Reduction in concrete tensile strength during fire exposure.tiff

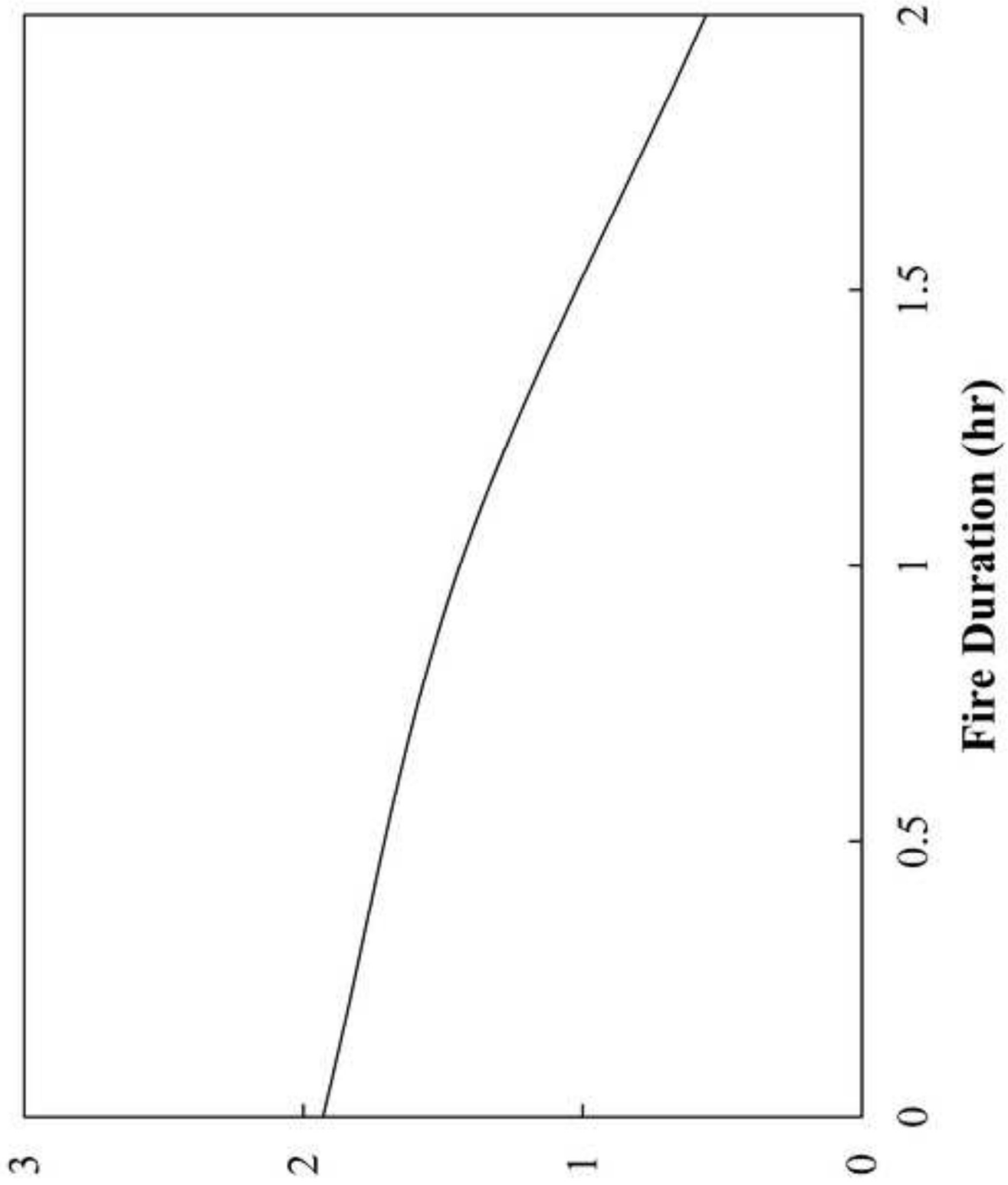

Figure 13
Click here to download Figure: 13- Reduction of shear capacity of B501 during fire.tiff

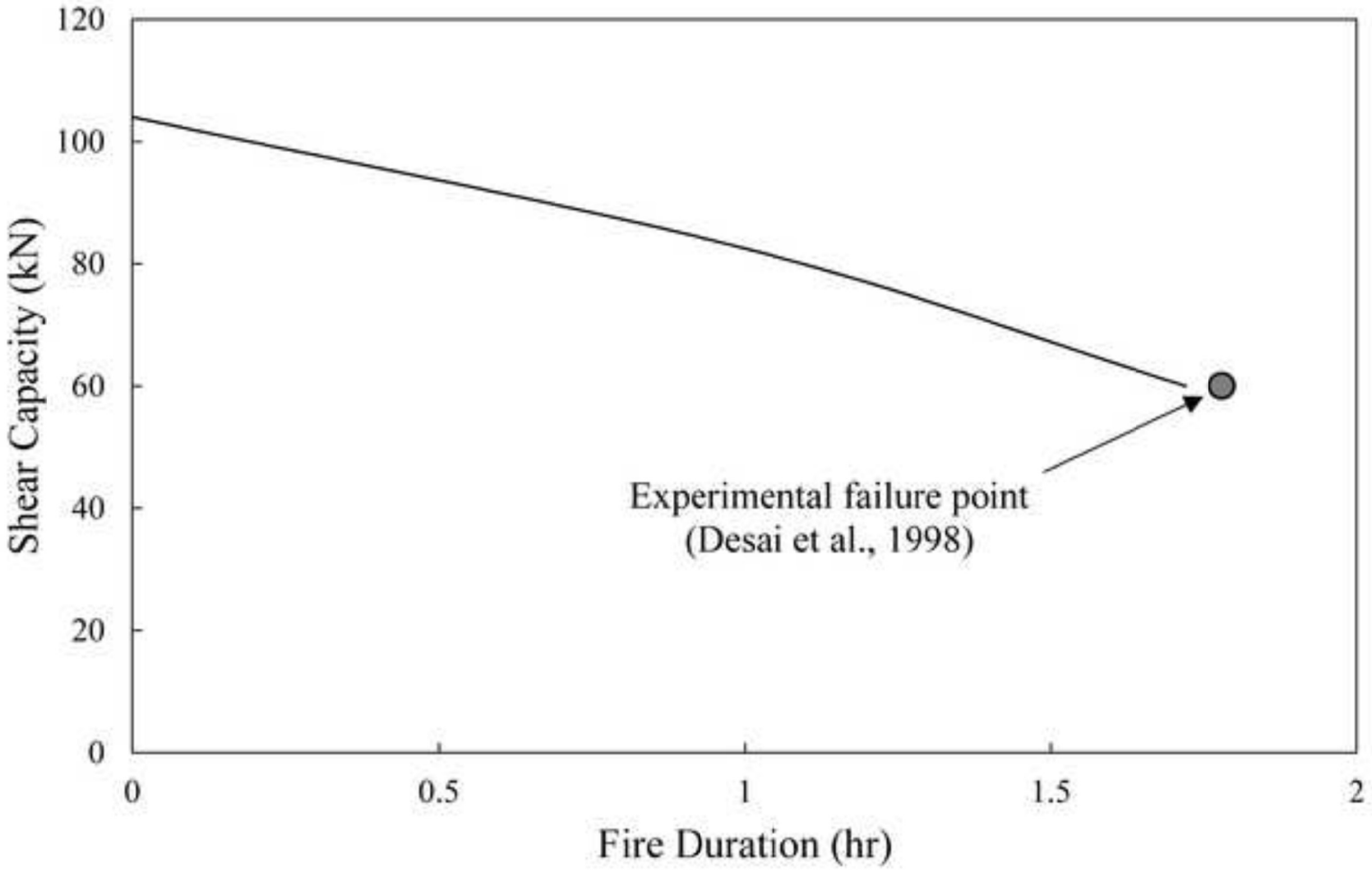

Figure 14
Click here to download Figure: 14- Shear capacity predictions using the proposed method.tiff

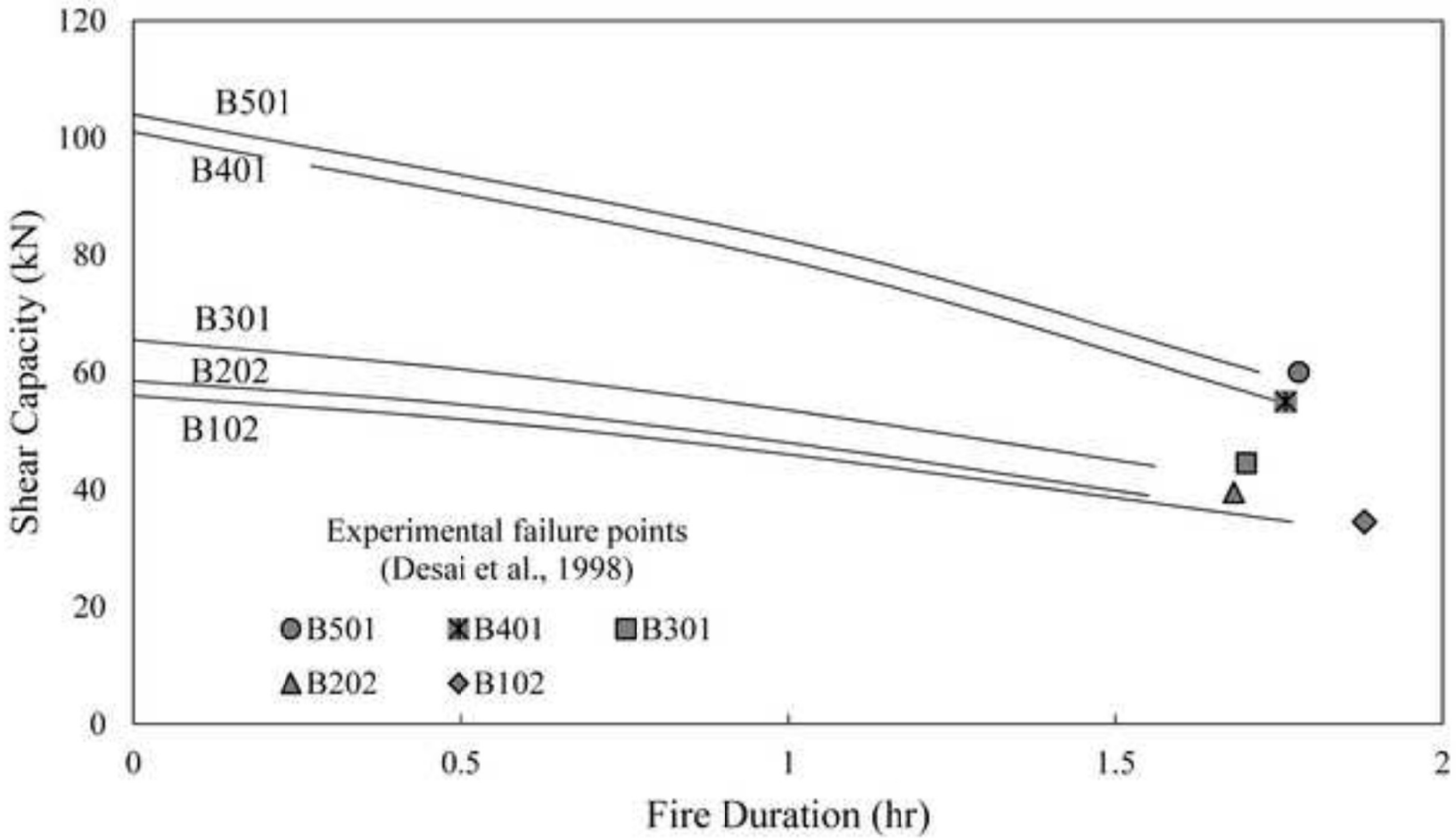

Figure 15
Click here to download Figure: 15-Comparison between predictions of the proposed method and experimental results by Desai (1998).tiff

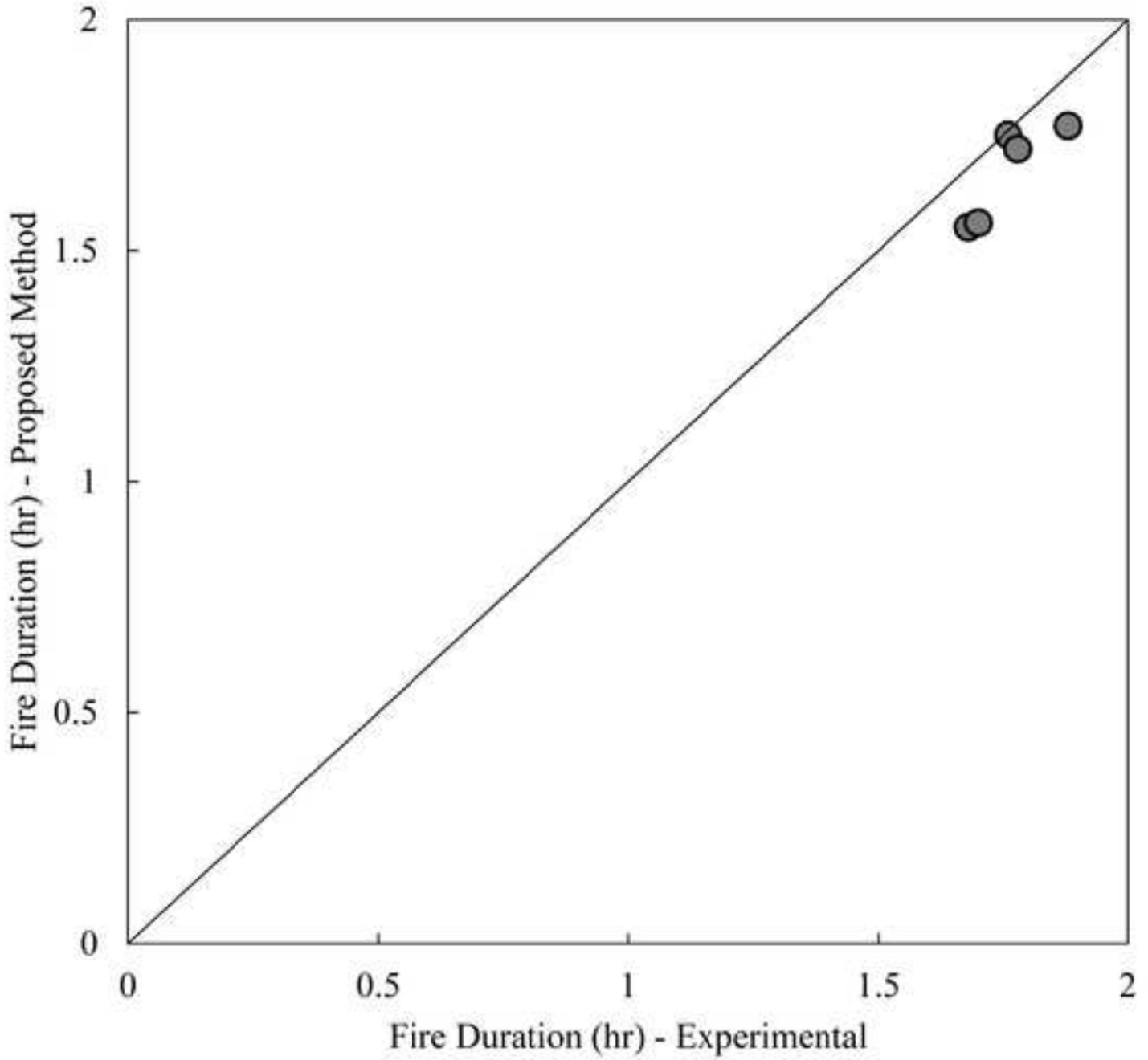

Figure 16
Click here to download Figure: 16- Comparison of the shear capacity predicted using the proposed method and the model by Hsu et al. (2008).tiff

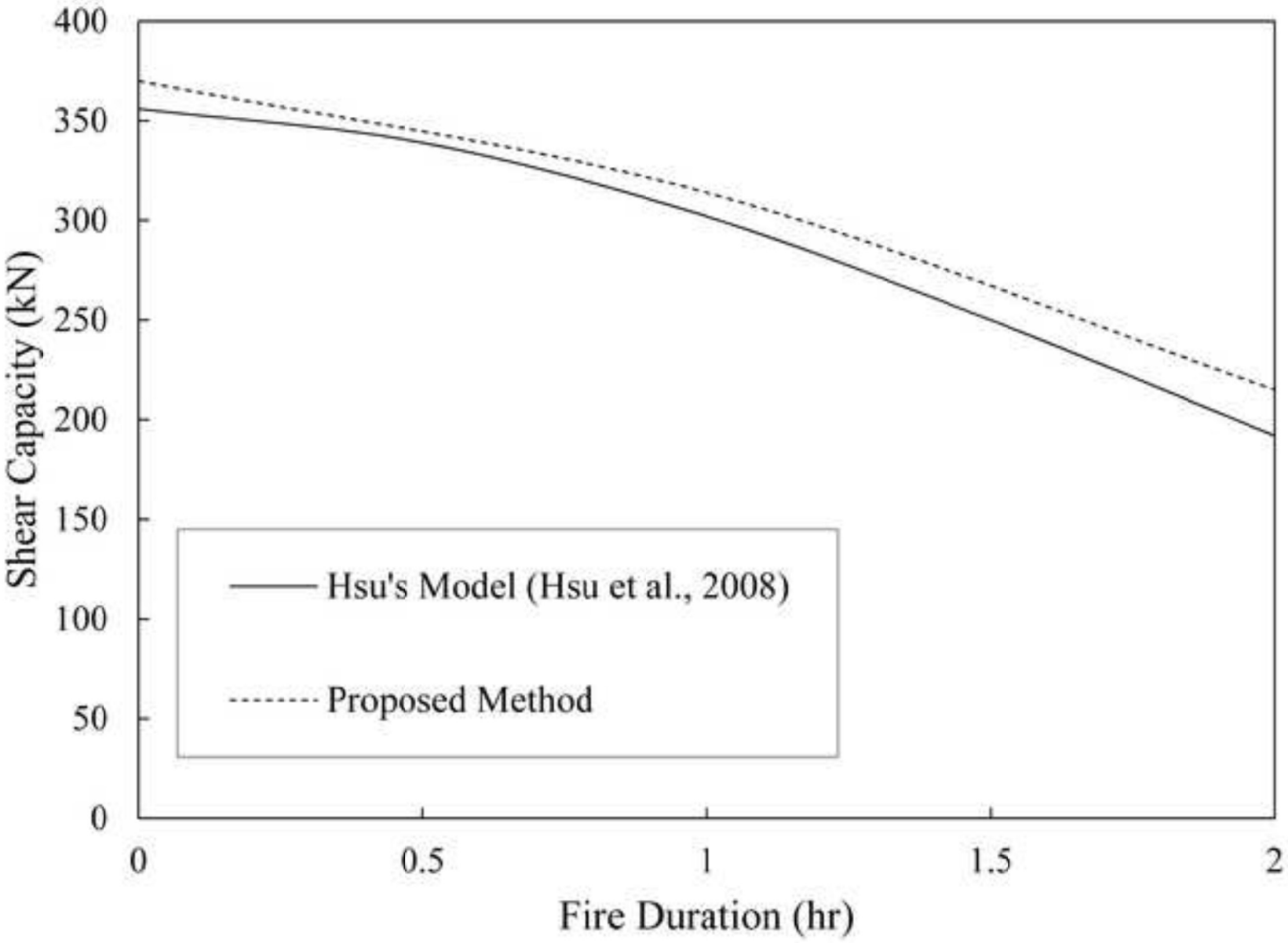

Figure 17
Click here to download Figure: 17- Effect of web reinforcement ratio on shear capacity during fire exposure.tiff

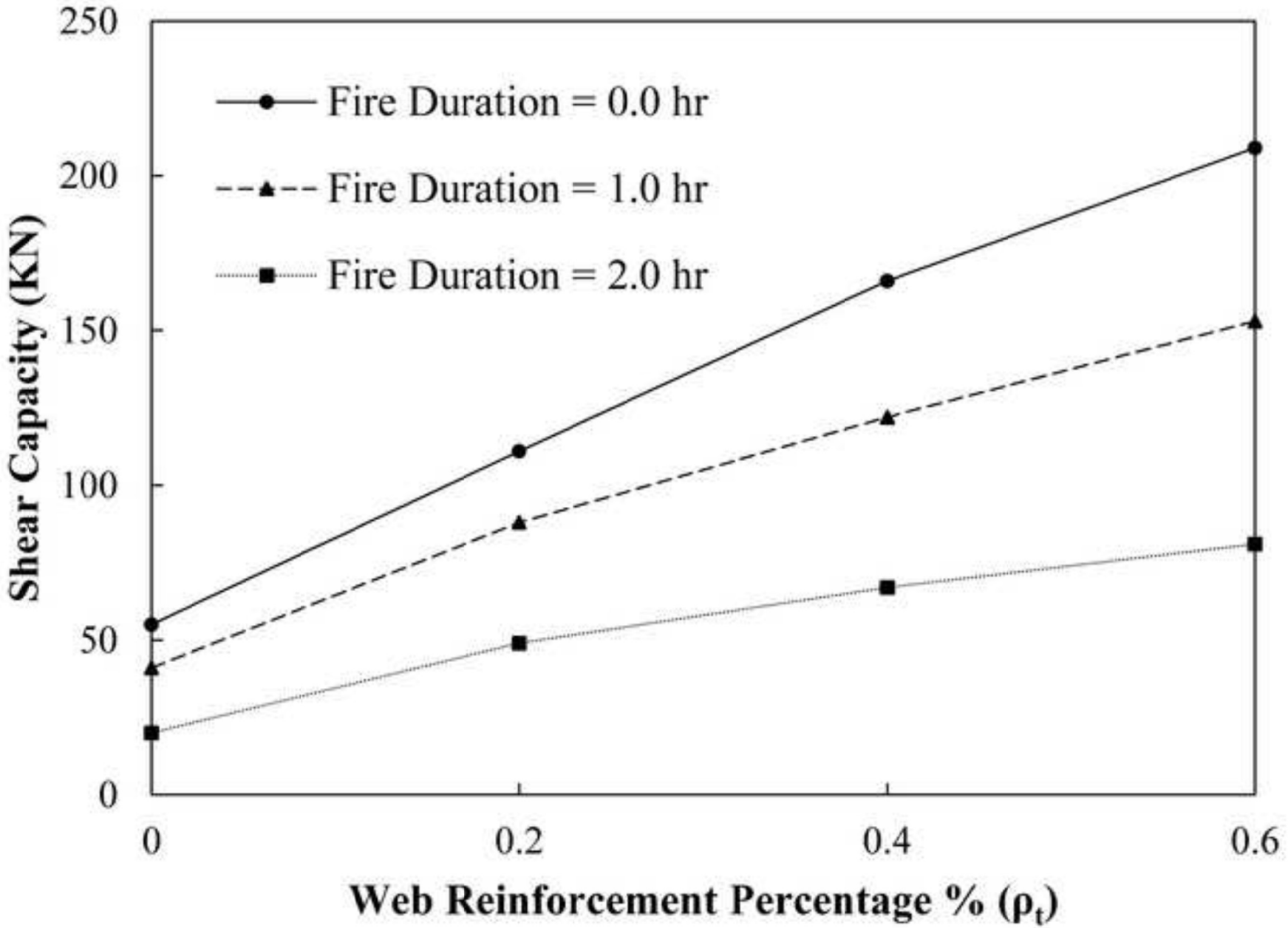

Figure 18
Click here to download Figure: 18- Effect of fire duration on the shear capacity for different web reinforcement ratios1.tiff

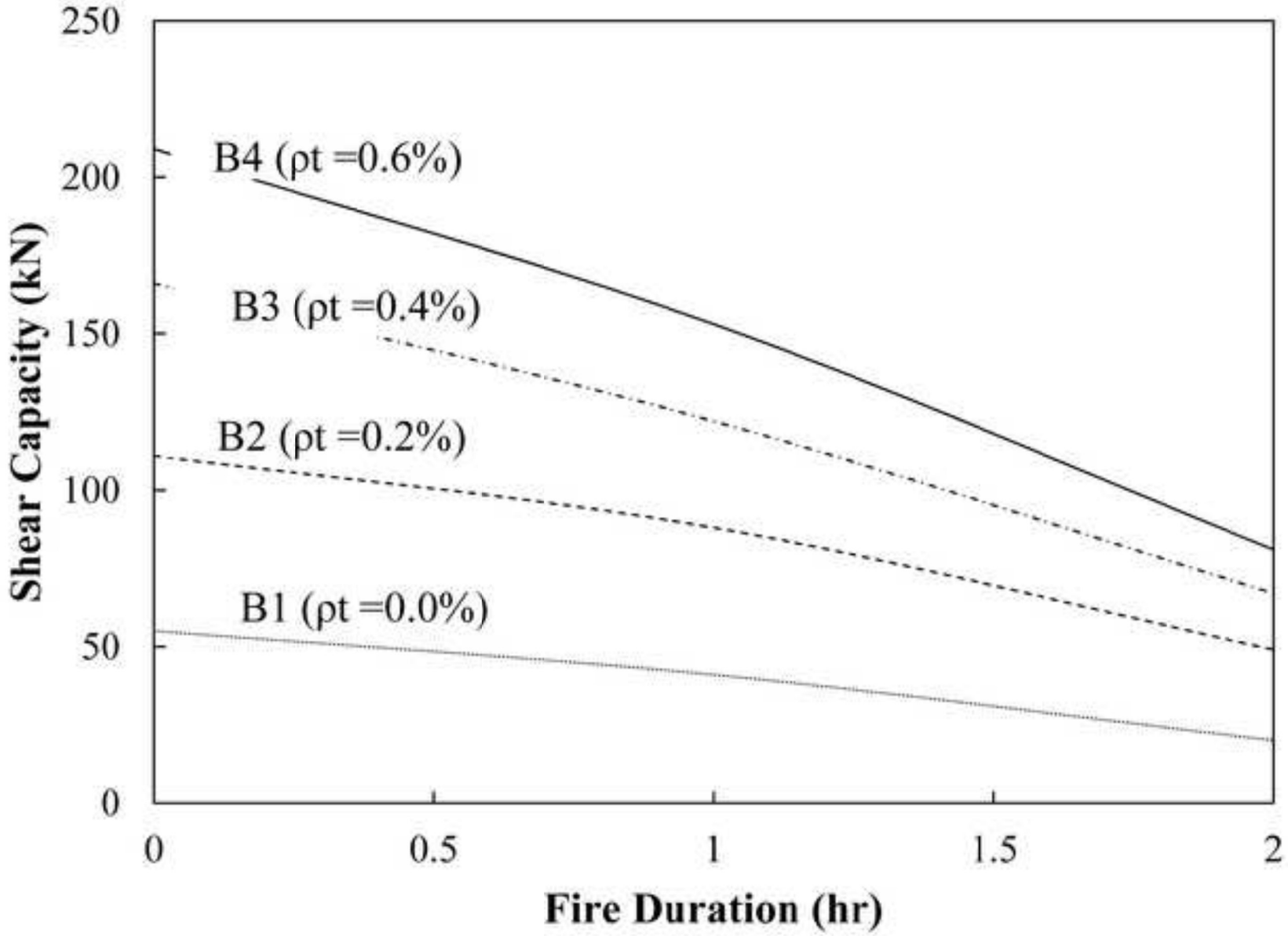

Figure 19
Click here to download Figure: 19-Effect of fire duration on the shear capacity for different longitudinal RFT ratios.tiff

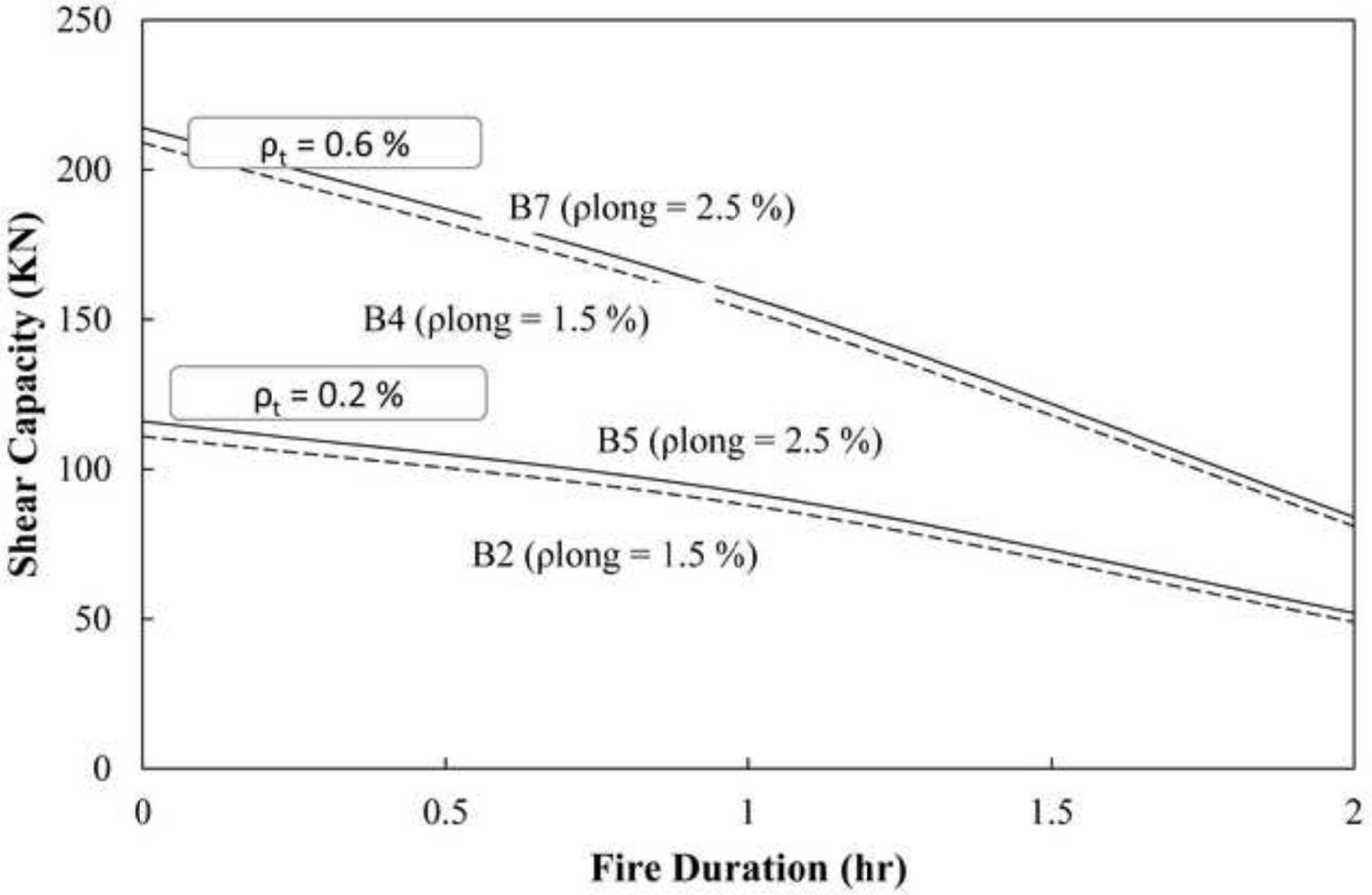

Figure 20
Click here to download Figure: 20-Effect of fire duration on the shear capacity for different concrete covers.tiff

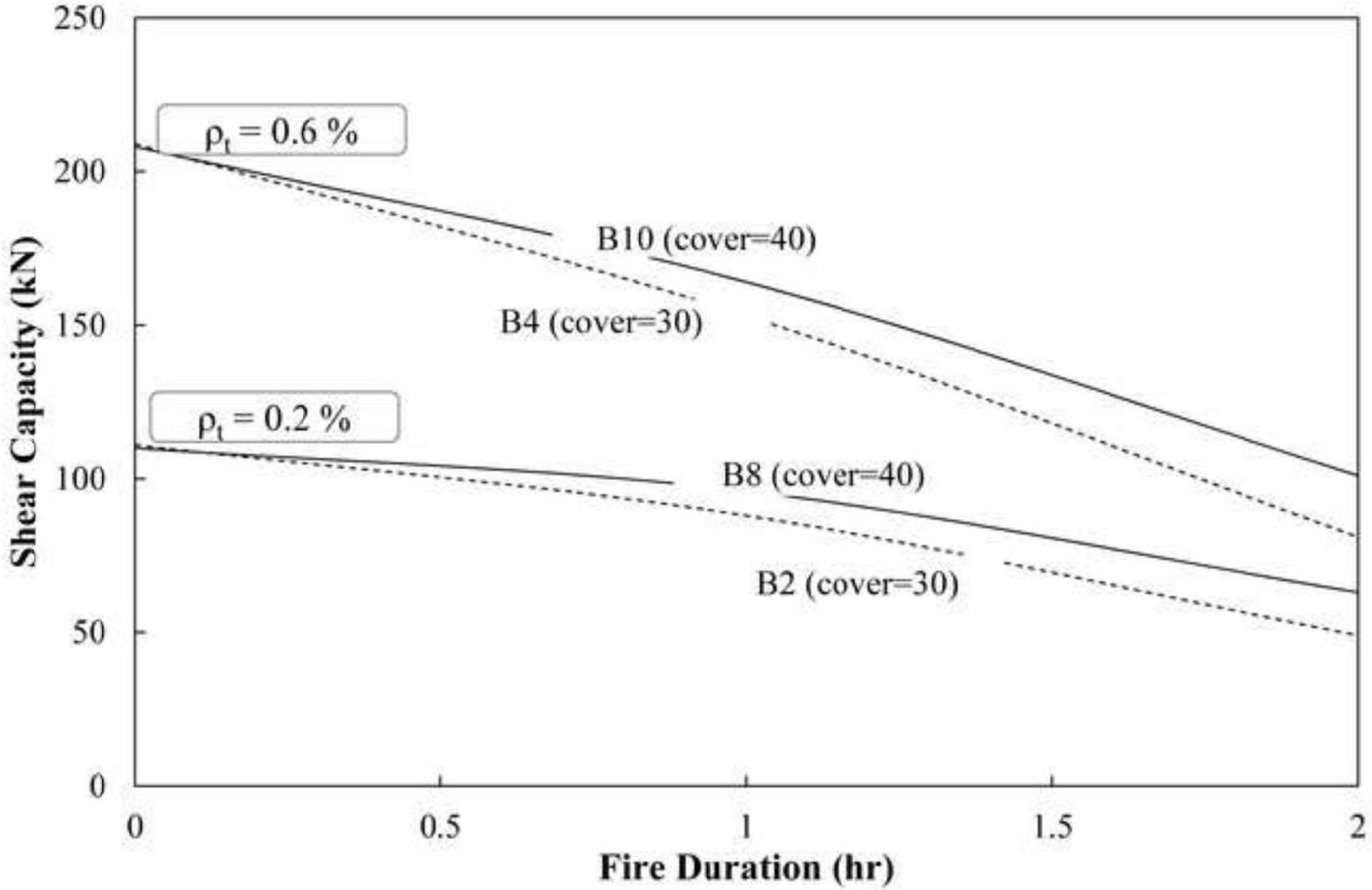

Figure 21
Click here to download Figure: 21-Effect of fire duration on the shear capacity for different beam heights..tiff

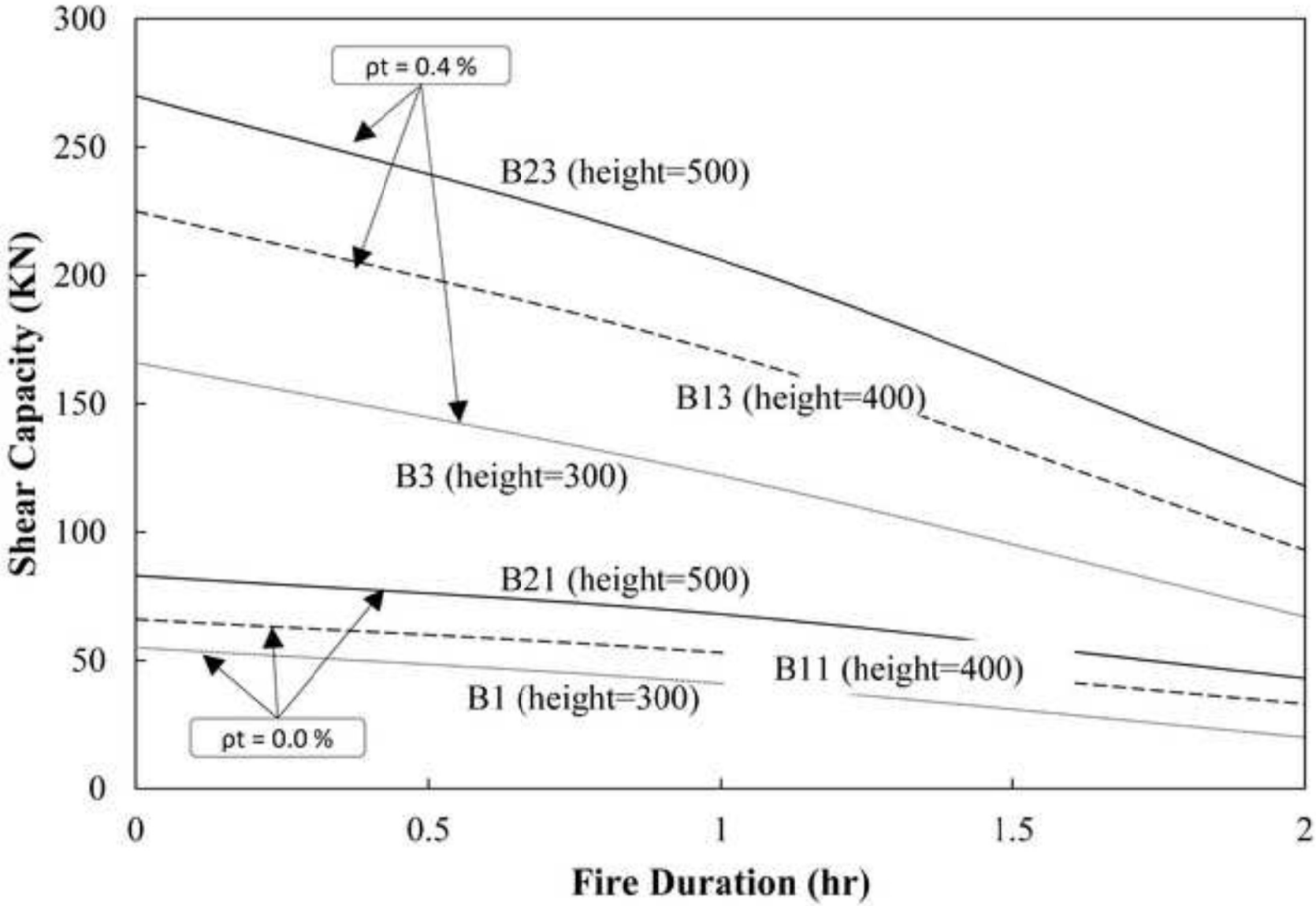

Figure 22
Click here to download Figure: 22-Effect of fire duration on the shear capacity for different beam widths.tiff

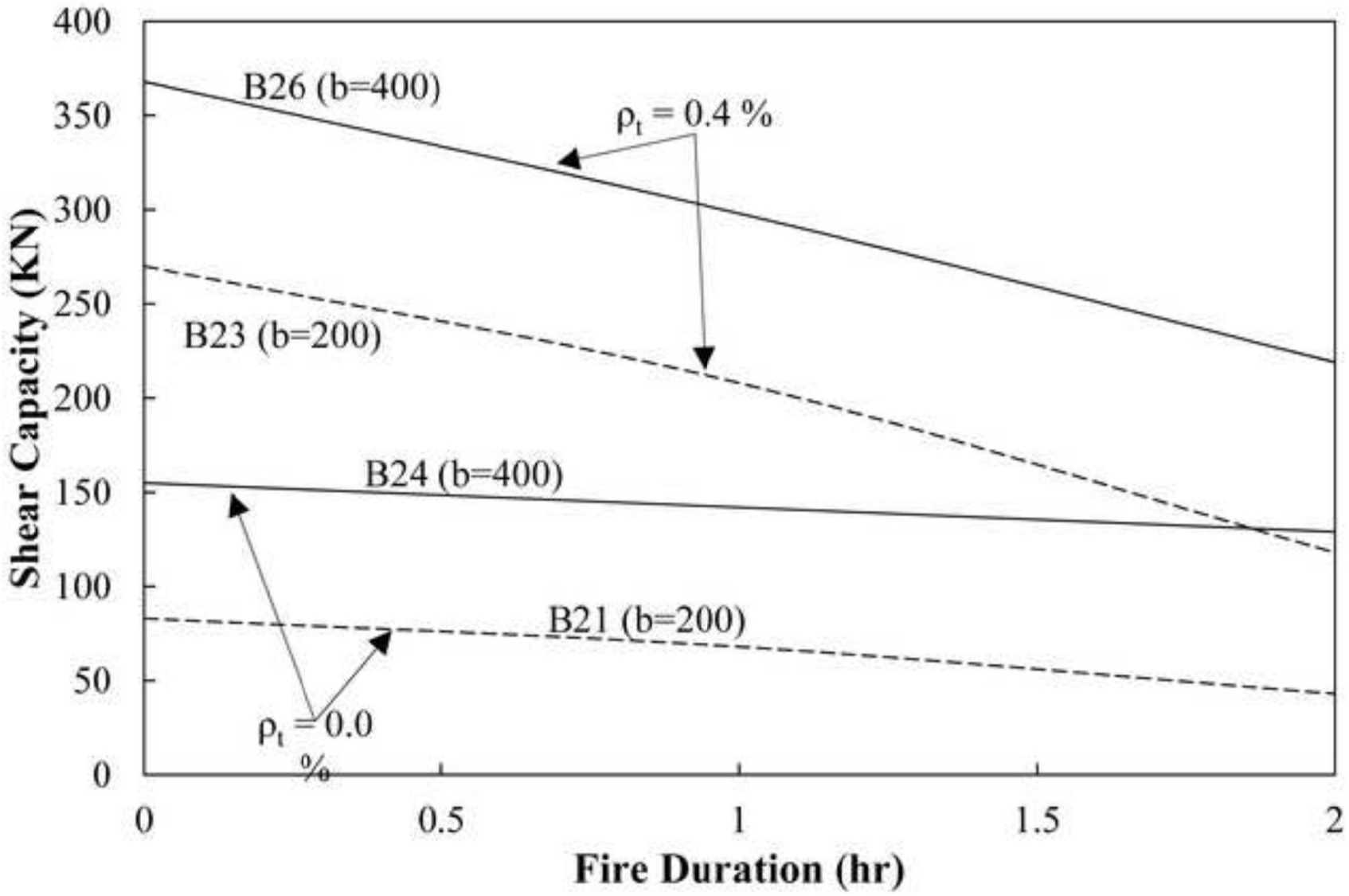

Figure 23
Click here to download Figure: 23- Effect of fire duration on the shear capacity for different concrete strengths..tiff

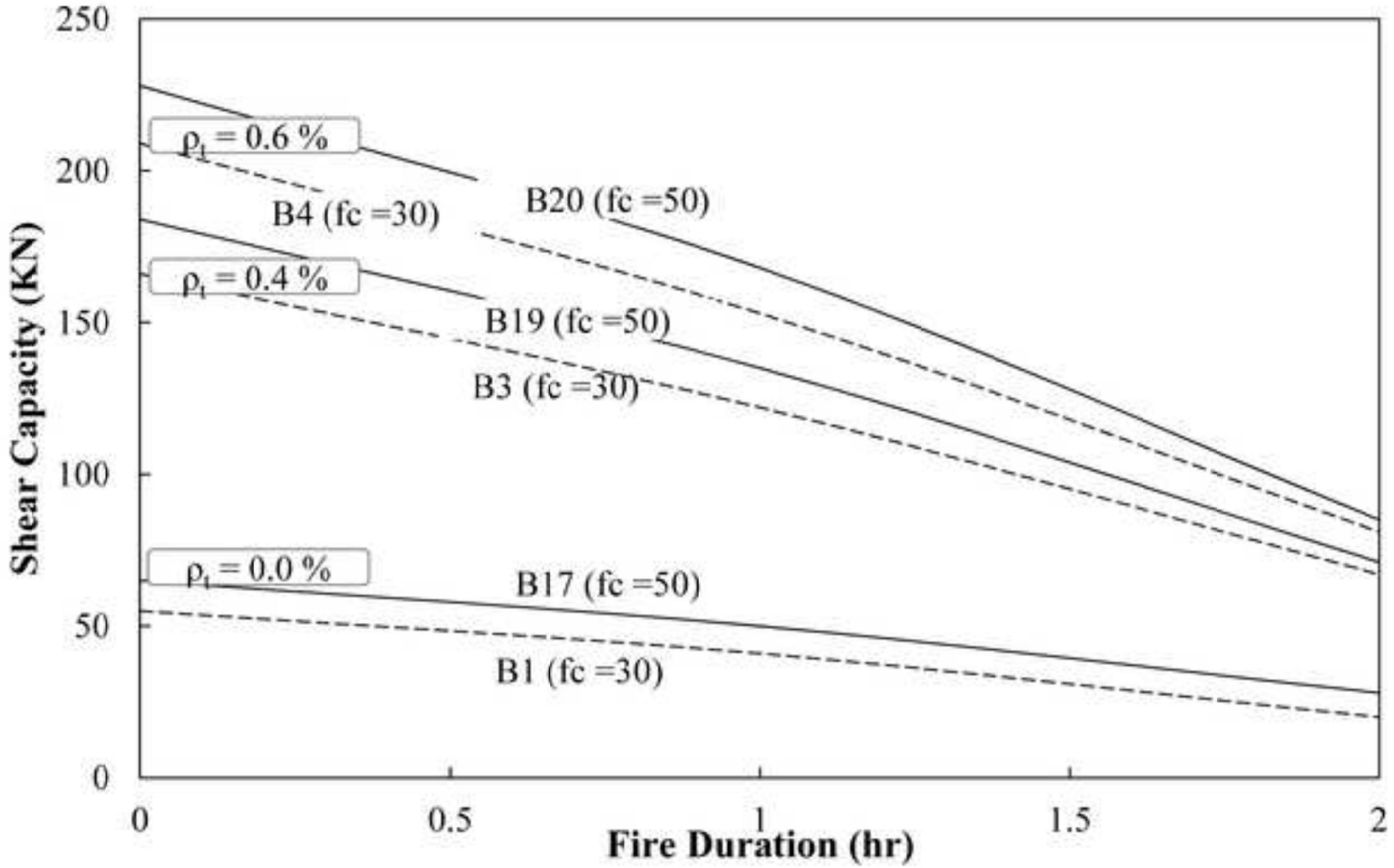

List of Abbreviations and Symbols

b	cross-section width
B_n	Beam designation number "n"
C_c	specific heat capacity.
E_s	initial modulus of elasticity of steel at ambient temperature
E_T	initial modulus of elasticity of steel at elevated temperatures
f'_c	compressive strength for concrete at ambient temperature
f_y	yield strength of steel bars at ambient temperature
f'_{cT}	reduced compressive strength at elevated temperatures
f_t	tensile strength for concrete at ambient temperature
f_{tT}	reduced tensile strength at elevated temperatures
f_{yT}	reduced yield strength of reinforcing bars at elevated temperatures
h	cross-section height
k_c	thermal conductivity.
T	fire temperature in degree Celsius
V_a	volume fraction of aggregates

ε_{th}	unrestrained thermal strain in concrete
ε_{tot}	total concrete strain at elevated temperatures
ε_{tr}	concrete transient strain
ε_{ot}	strain at maximum stress at elevated temperatures
ε_{o3}	transient creep strain for initial stress of $0.3\ f'_c$
ρ_l	longitudinal reinforcement ratio
ρ_t	transverse reinforcement ratio